The Astrophysical Journal Supplement Series, 143:73–111, 2002 November
© 2002. The American Astronomical Society. All rights reserved. Printed in U.S.A.

NEAR-INFRARED AND OPTICAL MORPHOLOGY OF SPIRAL GALAXIES[1]

Paul B. Eskridge,[2,3] Jay A. Frogel,[2,4,5,6] Richard W. Pogge,[2,4] Alice C. Quillen,[4,7] Andreas A. Berlind,[8] Roger L. Davies,[9] D. L. DePoy,[2,4] Karoline M. Gilbert,[2] Mark L. Houdashelt,[10] Leslie E. Kuchinski,[4,11] Solange V. Ramírez,[4,12] K. Sellgren,[2,4] Amelia Stutz,[2] Donald M. Terndrup,[2,4] and Glenn P. Tiede[4,13]

Received 2002 March 4; accepted 2002 June 16

ABSTRACT

We announce the initial release of data from the Ohio State University (OSU) Bright Spiral Galaxy Survey, a *BVRJHK* imaging survey of a well-defined sample of 205 bright, nearby spiral galaxies. We present *H*-band morphological classification on the Hubble sequence for the OSU Survey sample. We compare the *H*-band classification to *B*-band classification from our own images and from standard galaxy catalogs. Our *B*-band classifications match well with those of the standard catalogs. On average, galaxies with optical classifications from Sa through Scd appear about one T type earlier in the *H* band than in the *B* band, but with large scatter. This result does not support recent claims made in the literature that the optical and near-IR morphologies of spiral galaxies are uncorrelated. We present detailed descriptions of the *H*-band morphologies of our entire sample, as well as *B*- and *H*-band images for a set of 17 galaxies chosen as type examples and *BRH* color-composite images of six galaxies chosen to demonstrate the range in morphological variation as a function of wavelength.

Subject headings: galaxies: fundamental parameters — galaxies: general — galaxies: spiral — galaxies: statistics — galaxies: structure — infrared: galaxies

1. INTRODUCTION

Galaxy morphology has been a cornerstone of extragalactic research even before the discovery of the extragalactic nature of the nebulae (e.g., Parsons 1850). Detailed morphological classification of galaxies, in the modern sense, dates to the work of Hubble (1936), who established the now classic tuning-fork diagram for galaxy morphology. Since then there have been a number of modifications of this basic classification scheme. Sandage (1961) described the sequence in substantially more detail than did Hubble (1936). De Vaucouleurs (1959) presents a scheme that accounts for inner ring and spiral structure, as well as strong (SB) and weak (SAB) bar classes. A later version (de Vaucouleurs, de Vaucouleurs, & Corwin 1976) introduces the numerical "T-type" coding for morphology. This scheme is described in its most modern form in de Vaucouleurs et al. (1991, hereafter RC3). Van den Bergh (1976 and references therein) introduced the DDO luminosity classification scheme that relates the surface brightness and the appearance of spiral arms with the absolute luminosity of the galaxy. Elmegreen & Elmegreen (1982) created a classification scheme for the degree of structure seen in the spiral arms of galaxies, ranging from flocculent (arm class 0) to grand design (arm class 12). Buta (1986) and Buta (1995) added a much more detailed classification scheme for resonance rings following the general precepts of de Vaucouleurs (1959). The most significant departure from the basic Hubble scheme is that proposed by Morgan (1958) and given in its final form by Morgan, Kayser, & White (1975). This scheme is essentially a one-dimensional classification based on the degree of concentration of light, with a secondary "form" parameter to distinguish amongst gross galaxy types.

A common property and, therefore, a common weakness of all these schemes has been the nearly exclusive use of *B*-band plate material for galaxy classification (although see Zwicky 1955 and Schweizer 1976 for early work on multiwavelength morphology). This constrains existing classification schemes in two major ways. First, as classification has been done primarily in the *B* band, it is very sensitive to the distribution of blue stars and dust. This is particularly unfortunate for the study of late-type galaxies, as the distribution of the young, blue stars and the dust can be very different from the distribution of the total baryonic mass. Second, although well-exposed plates, taken under good seeing conditions, can offer excellent spatial resolution, plates are poor photometric detectors and have a very limited dynamic range. Thus, for instance, it is possible to miss features such as nuclear bars in classification plates that are

[1] Based partially on observations obtained at the Cerro Tololo Inter-American Observatory, operated by the Association of Universities for Research in Astronomy (AURA), Inc., under cooperative agreement with the National Science Foundation.

[2] Department of Astronomy, The Ohio State University, Columbus, OH 43210.

[3] Department of Physics and Astronomy, Minnesota State University, Mankato, MN 56001; paul.eskridge@mnsu.edu.

[4] Visiting Astronomer, Cerro Tololo Inter-American Observatory.

[5] Visiting Senior Scientist, Lawrence Berkeley National Laboratory, Berkeley, CA 94720.

[6] Present address: NASA Headquarters, Code S, 300 E Street SW, Washington, DC 20546.

[7] Department of Physics and Astronomy, University of Rochester, Rochester, NY 14627.

[8] Department of Astronomy and Astrophysics, University of Chicago, Chicago, IL 60637.

[9] Department of Physics, South Road, University of Durham, Durham DH1 3LE, England.

[10] Department of Physics and Astronomy, Johns Hopkins University, Baltimore, MD 21218.

[11] NASA/IPAC, California Institute of Technology, MS 100-22, Pasadena, CA 91125.

[12] Astronomy Department, California Institute of Technology, MS 105-24, Pasadena, CA 91125.

[13] Department of Astronomy, University of Florida, Gainesville, FL 32601.

deeply exposed in order to reveal the structure of spiral arms in the outer disk (see Eskridge et al. 2000 for a discussion of this effect).

The advent of two-dimensional near-infrared (near-IR) detectors has resulted in numerous efforts (e.g., Hackwell & Schweizer 1983; Thronson et al. 1989; Block & Wainscoat 1991; Block et al. 1994; Block & Puerari 1999) to compare galaxy morphology in the optical and near-IR. These studies revealed that there can be substantial differences between the optical and near-IR morphologies of spiral galaxies. Indeed, Block & Puerari (1999) assert that there is no correlation between the optical and near-IR classifications of spirals. The main problem with these studies is that they deal with single galaxies or, at most, small samples of objects. In fact, the lack of a large, well-defined sample of multiwavelength digital imaging of spirals prompted the creation of the Ohio State University (OSU) Bright Spiral Galaxy Survey.

We believe that classification in both the optical and near-IR of a large, statistically complete sample of spirals is an important step in our understanding of the physical morphology of galaxies as a function of wavelength. The astrophysical motivation for such a comparison is that very different sorts of stars dominate the emission from spiral galaxies at optical (*B* band) and near-IR wavelengths. In the optical, the regions of current massive star formation, typically associated with the spiral arms, will dominate. Further, the absorbing effect of interstellar dust is substantial in the optical, and this material is also typically concentrated along the spiral arms. In the near-IR, the flux is dominated by light from old giants. There can be significant contributions from young supergiants, but this effect appears to be small in all but the most extreme situations (Rhoads 1998).

A number of recent studies have attempted to classify galaxies in some sort of automated way (e.g., Abraham et al. 1994; Odewahn et al. 1996, 2002; Naim, Ratnatunga, & Griffiths 1997). Such efforts, while promising, have mainly been devoted to classification at the very simplest level: determining if a given extended object is a pure spheroid, a disky system, or peculiar. There have been pioneering efforts aimed at objective bar and spiral structure classification (e.g., Abraham et al. 1999; Odewahn et al. 2002), and such efforts have largely been directed at studying high-redshift galaxy samples. This is appropriate as such samples are very large (thousands of objects) and each galaxy is typically only a few resolution elements in diameter. Detailed classification of well-resolved galaxies is still the provenance of "expert classifiers." A landmark study of the classification biases of different "expert classifiers" (Naim et al. 1995) reveals that different classifiers are in general agreement with one another but typically have a scatter of about one T type. Whether this is good or bad agreement is, of course, a subjective decision. We believe it is good enough, given the underlying purpose of morphological classification. Although descriptive classification is not physical, it is an essential starting point for a physical classification scheme: morphology is akin to species taxonomy. Species taxonomy is not genetics, but it is an essential guide to asking relevant questions in genetics (e.g., Mayr 1942).

In this paper we present the Ohio State University Bright Spiral Galaxy Survey sample; a large, statistically well-defined sample of bright nearby spiral galaxies. While previous multiobject samples (most notably that of Frei et al. 1996) have been a great boon for many sorts of projects, none of these samples cover a wavelength range from the optical through the near-IR and are both large and selected according to a well-defined set of criteria. We hope that the availability of the OSU Survey data will be of use to the community. In § 2 we describe the survey selection and data taking procedure. We present statistical results of the comparison of the *B*- and *H*-band morphologies of the sample in § 3 and give notes on the *H*-band morphologies in § 4. In § 5 we discuss some implications of our results and suggest promising areas for future research.

2. THE OSU BRIGHT SPIRAL GALAXY SURVEY

The Ohio State University Bright Spiral Galaxy Survey comprises deep, photometrically calibrated *BVRJHK* images of 205 spiral galaxies selected from the RC3 according to the following criteria: $0 \leq T \leq 9$; $M_B \leq 12$; $D \leq 6'.5$; $-80^\circ < \delta < +50^\circ$ (due to the pointing limits of the CTIO 1.5 m and Perkins 1.8 m reflectors). We have been unable to obtain near-IR data for 12 galaxies from the defined sample that are south of $\delta = -25^\circ$ (we have optical data for six of these galaxies). Figure 1 shows histograms of RC3 T types for all galaxies in the RC3 with $M_B \leq 12$ and RC3 ellipticity <0.5 (*solid histogram*) and for the OSU Sample as defined above (*dotted histogram*). It is clear from this figure that our diameter and declination cutoffs do not impose any morphological selection bias on the OSU Survey.

We obtained the data for the survey in a large number of observing runs with six different telescopes of apertures between 0.9 and 2.4 m, in both hemispheres in the period 1993–2000. The *JHK* data were obtained mainly with the 1.8 m Perkins reflector of the Lowell Observatory and the CTIO 1.5 m, with some additional data from the 2.4 m Hiltner telescope of the MDM Observatory. We used OSIRIS (DePoy et al. 1993) at the 1.8 m and the 1.5 m. We also used CIRIM[14] at the 1.5 m. The data from the 2.4 m were taken with TIFKAM (Pogge et al. 1998). The *BVR* data were obtained mainly with the 1.8 m Perkins reflector and the CTIO 0.9 m, with additional data from the USNO 1.1 m Hall Telescope of the Lowell Observatory, the 1.3 m McGraw-Hill telescope of the MDM Observatory, and the CTIO 1.5 m. A large number of imaging cameras and detectors were used to obtain the *BVR* imaging.

For the near-IR imaging, our typical observing strategy was as follows: We would obtain a series of short (1–20 s) observations with no readout or dither (a stack). We would then read out the stack, dither the telescope, and take another stack. We would then chop by a distance comparable to the field of view and take a similar set of dithered sky observations. The total on-source integration time per galaxy in *J* and *H* are typically 10–15 minutes. In *K* we observed somewhat longer, generally between 20 and 30 minutes. For the optical imaging, our typical strategy was to obtain three images per filter, with total integration times of 20–30 minutes in *B*, 10–15 minutes in *V*, and 5–10 minutes in *R*. As we had many nights of observing time that were nonphotometric, we adopted a strategy of obtaining deep images on nonphotometric nights and using photometric nights to obtain short integrations ("snapshots") of large numbers of galaxies to calibrate our deep images. Our

[14] See http://www.ctio.noao.edu/instruments/ir_instruments/cirim/cirim.html.

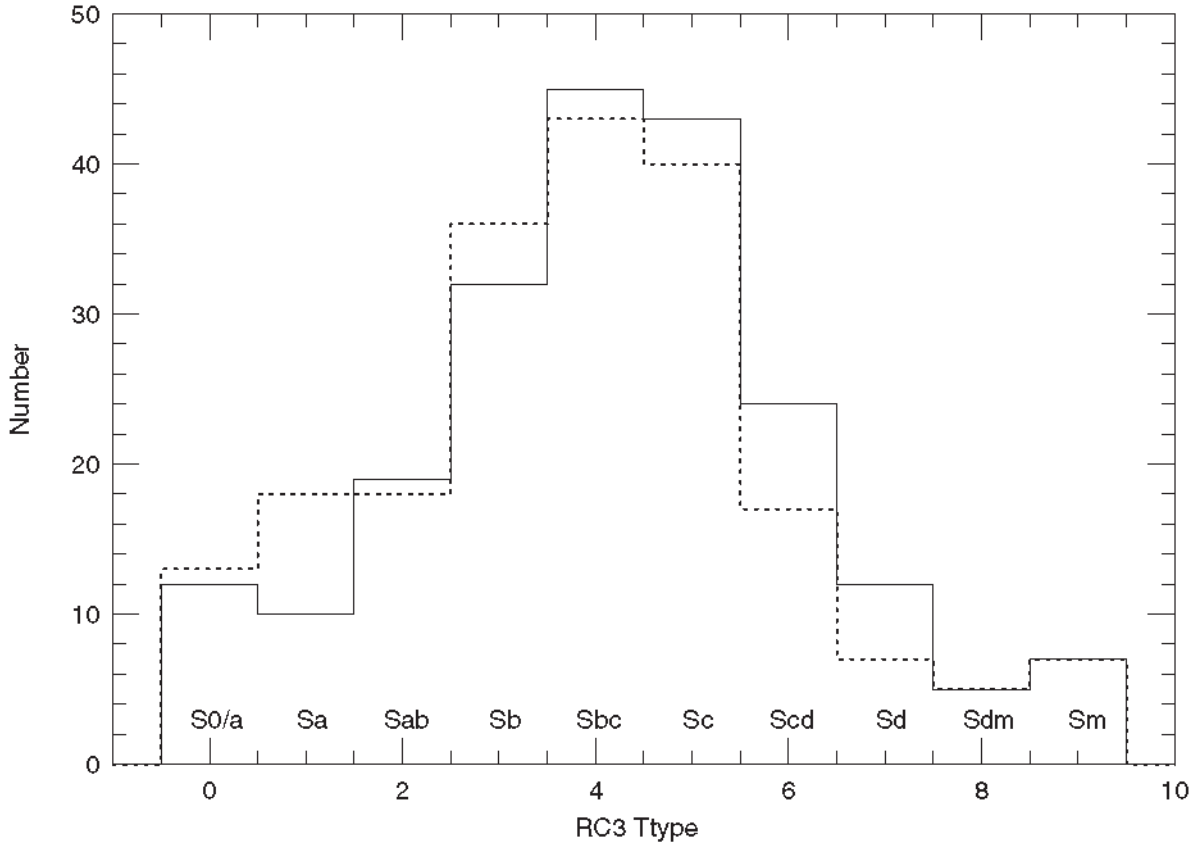


FIG. 1.—Histograms of the distribution of RC3 T types for all spirals in the RC3 with $M_B \leq 12$ and ellipticity <0.5 (*solid histogram*) and for the OSU Sample (*dotted histogram*). The coding of RC3 T type with Hubble stage is shown along the bottom of the figure.

data are unavoidably heterogeneous, having been obtained at many telescopes, with many different instruments, by many different observers, and under a wide range of sky conditions. However, the approximate limiting surface brightnesses of typical OSU Survey data are $B_{\rm lim} \approx 26$ mag arcsec^{-2} and $H_{\rm lim} \approx 20$ mag arcsec^{-2}.

Information about the OSU Survey is available on-line.[15] With the acceptance of this paper for publication, we shall make the uncalibrated *B* and *H* images available as an Early Data Release.[16] We plan on making the entire calibrated *BVRJHK* data set publicly available when we are satisfied with the photometric calibration. Anyone who is interested in using data that have not been publicly released yet is encouraged to contact one of the first three authors.

3. *H*- AND *B*-BAND MORPHOLOGY

In Table 1 we present the sample. Column (1) gives the NGC, IC, ESO, or Anon designations of the galaxies in the sample. In columns (2) and (3) we give the morphological types from the RC3 and the Carnegie Atlas of Galaxies (Sandage & Bedke 1994, hereafter CAG). Columns (4) and (5) present our *B*- and *H*-band classifications. Our *B*-band classification follows the precepts laid out in the RC3 and CAG and is generally closer to those of the RC3. Our *H*-band classification follows these same general precepts, but with a number of differences driven by the nature of the *H*-band morphology of spirals. The classic prescription for the classification of spirals involves three observables: the bulge-to-disk ratio; the pitch angle of the spiral arms; and the degree of resolution (or knottiness) of the arms. For two of these three observables, there is a clear bias toward an earlier classification from near-IR images. In near-IR images, the bulge is more prominent, and the spiral arms are less knotty than they appear in optical images. It is not obvious that the pitch angle of the spiral arms should change systematically from the optical to the near-IR. Block & Puerari (1999) find substantially different pitch angles in optical and near-IR images of a small sample of spirals, but they do not see evidence for any systematic trend. As the degree of resolution in the arms of even very late type galaxies is substantially lower in the *H* band than in the optical, the essential features in determining the *H*-band Hubble stage are the bulge-to-disk ratio and the pitch angle of the spiral arms.

As we discussed in § 1, the optical and near-IR emission from spirals is dominated by different populations of stars and subject to different levels of dust absorption. Thus, structures that are dominated by older stellar populations should be more prominent in the near-IR than the in optical. This has the consequence that the bar fraction in the near-IR is significantly higher than it is in the *B* band (Eskridge et al. 2000). It should also cause the observed bulge-to-disk ratio to be higher in the near-IR than in the optical. This should tend to drive near-IR morphological

[15] See http://www.astronomy.ohio-state.edu/~survey/.
[16] See http://www.astronomy.ohio-state.edu/~survey/EDR/index.html.

TABLE 1

SAMPLE CLASSIFICATION

Name (1)	RC3 Type (2)	CAG Type (3)	OSU *B* Type (4)	OSU *H* Type (5)
NGC 150	SB(rs)b	Sbc(s)II pec	SABb	SBb
NGC 157	SAB(rs)bc	Sc(s)II–III	SBbc	Sbc
NGC 210	SAB(s)b	Sb(rs)I	(R)Sab	(R)SB0/a
NGC 278	SAB(rs)b	Sbc(s)II.2	Sab	Sb
NGC 289	SB(rs)bc	SBbc(rs)I–II	SB(r)bc	SB(r)ab
NGC 428	SAB(s)m	Sc(s)III	SABd	SBm
NGC 488	SA(r)b	Sab(rs)I	Sa	Sa
NGC 578	SAB(rs)c	Sc(s)II	SABcd	SBc
NGC 613	SB(rs)bc	SBb(rs)II	SBc	SB(r)bc
NGC 625	SB(s)m? sp	Amorph/ImIII	Sm	Sm
NGC 685	SAB(r)c	SBc(rs)II	SBcd	SBcd
NGC 779	SAB(r)b	Sb(rs)I–II	Sab	SAB(r)b
NGC 864	SAB(rs)c	Sbc(r)II–III/SBbc(r)II–III	SABc	SBb
NGC 908	SA(s)c	Sc(s)I–II	Sb	Sc
NGC 986	(R'_1)SB(rs)b	SBb(rs)I–II		
NGC 988	SB(s)cd:			SBcd
IC 239	SAB(rs)cd		SABc	SBc
NGC 1003.....	SA(s)cd		Sdm	Scd? (edge-on)
NGC 1042.....	SAB(rs)cd	Sc(rs)I–II	SABbc	SABc
NGC 1058.....	SA(rs)c	Sc(s)II–III	Sab	Sa
NGC 1073.....	SB(rs)c	SBc(rs)II	SB(r)c	SB(r)ab
NGC 1084.....	SA(s)c	Sc(s)II.2	Sbc	Sb
NGC 1087.....	SAB(rs)c	Sc(s)III.3	SBd	SBd
NGC 1187.....	SB(r)c	Sbc(s)II	SBc	SB(r)b
NGC 1241.....	SB(rs)b	SBbc(rs)I.2	SAB(r)bc	SB(r)ab
NGC 1255.....	SAB(rs)bc	Sc(s)II		
NGC 1300.....	(R′SB(rs)bc	SBb(s)I.2	SBb	SBb
NGC 1302.....	(R)SB(r)0/a	Sa	(R)SABa	SB0
NGC 1309.....	SA(s)bc:	Sc(s)II	Scd	SABb
NGC 1317.....	SAB(r)a	Sa(s)	SB(r)a	SB0
NGC 1350.....	(R'_1)SB(r)ab	Sa(r)	(R)SAB(r)a	(R)SB(r)a
NGC 1371.....	SAB(rs)a	Sa(s)	SABab	SAB(r)a
NGC 1385.....	SB(s)cd	SBc	SBd	SBdm
NGC 1421.....	SAB(rs)bc:	Sc	Sd	Sc
NGC 1425.....	SA(rs)b	Sb(r)II		
NGC 1433.....	(R'_1)SB(rs)ab	SBb(s)I–II		
NGC 1493.....	SB(r)cd	SBc	SABc	SBd
NGC 1511.....	SAa: pec	Sc pec or Amorph	Sm?	SBd? (edge-on)
NGC 1559.....	SB(s)cd	SBc(s)II.2	SBc	SBcd
NGC 1617.....	(R′SB(s)a	Sa(s)	Sa	(R)SAB0/a
NGC 1637.....	SAB(rs)c	SBc(s)II.3	Sbc	SBb (pec)
NGC 1703.....	SB(r)b		Sc	SABb
NGC 1792.....	SA(rs)bc	Sc(s)II	Scd	Sbc
NGC 1808.....	(R'_1)SAB(s)a	Sbc pec	SABb? pec	SBa
NGC 1832.....	SB(r)bc	SBb(r)I	SAB(r)c	SBab
NGC 1964.....	SAB(s)b	Sb(s)I–II	(R)SAB(r)b	(R)Sab
NGC 2090.....	SA(rs)c	Sc(s)II	SABb	Sb
NGC 2139.....	SAB(rs)cd	SBc	SBd	SBdm
NGC 2196.....	(R′)SA(s)a	Sab(s)I	Sa	S0/a
NGC 2207.....	SAB(rs)bc pec	Sc(s)I.2	S(r)b pec	SB0/a
NGC 2280.....	SA(s)cd	Sc(s)I.2	Sab	SBbc
NGC 2442.....	SAB(s)bc pec	SBbc(rs)II	SBc	SBbc
NGC 2559.....	SB(s)bc: pec		SABcd?	SBb
NGC 2566.....	(R′)SB(rs)ab: pec		SB(r)ab	(R)SBa
NGC 2775.....	SA(r)ab	Sa(r)	Sa	S0/a
A0908-08	SAB(rs)b: sp		Sc? (edge-on)	Sc? (edge-on)
NGC 2964.....	SAB(r)bc:	Sc(s)II.2	Sbc	SABb pec
NGC 3059.....	SB(rs)bc	SBc(s)III	SBcd	SBcd
NGC 3166.....	SAB(rs)0/a	Sa(s)	Sa	SB0
NGC 3169.....	SA(s)a pec	Sb(r)I–II tides	Sb	S0/a
NGC 3223.....	SA(s)b	Sb(s)I–II	Sb	Sa
NGC 3227.....	SAB(s) pec	Sb(s) (tides)	SABb	SBab
NGC 3261.....	SB(rs)b	SBab(rs)I–II	SAB(r)b	SB(r)a
NGC 3275.....	SB(r)ab	SBab(r)I	SB(r)ab	SB(r)ab

TABLE 1—*Continued*

Name (1)	RC3 Type (2)	CAG Type (3)	OSU *B* Type (4)	OSU *H* Type (5)
NGC 3319.....	SB(rs)cd	SBc(s)II.4	SBcd	SBd
NGC 3338.....	SA(s)c	Sbc(s)I–II	SAB(r)bc	SAB(r)b
NGC 3423.....	SA(s)cd	Sc(s)II.2	Sc	Sd
NGC 3504.....	(R)SAB(s)ab	Sb(s)/SBb(s)I–II	(R)SBab	(R)SB(r)a
NGC 3507.....	SB(s)b		SBb	SBb
NGC 3511.....	SA(s)c	Sc(s)II.8	Scd	SABbc
NGC 3513.....	SB(rs)c	SBc(s)II.2	SBcd	SBc
NGC 3583.....	SB(s)b	Sbc	SABc	SBc
NGC 3593.....	SA(s)0/a:	Sa pec	Sa	S0/a
NGC 3596.....	SAB(rs)c	Sbc(r)II.2	S(r)bc	SABb
NGC 3646.....	RING	Sbc(r)II pec	(R)Sb	SABab pec
NGC 3675.....	SA(s)b	Sb(r)II	SABab	SB(r)a
NGC 3681.....	SAB(r)bc	SBb(r)I–II	SAB(r)b	SB(r)0/a
NGC 3684.....	SA(rs)bc	Sc(s)II	SABc	SABb
NGC 3686.....	SB(s)bc	SBbc(s)II	SABbc	SBbc
NGC 3705.....	SAB(r)ab	Sb(r)I–II	S(r)b	SAB(r)ab
NGC 3726.....	SAB(r)c	Sbc(rs)II	SAB(r)c	SB(r)bc
NGC 3810.....	SA(rs)c	Sc(s)II	Sbc	SABbc
NGC 3877.....	SA(s)c:	Sc(s)II	Sc	Sbc? (edge-on)
NGC 3885.....	SA(s)0/a	Sa	Sa? pec	S0/a
NGC 3887.....	SB(r)bc	SBbc(s)II–III	SABbc	SBab
NGC 3893.....	SAB(rs)c	Sc(s)I.2	Sbc	SABbc
NGC 3938.....	SA(s)c	Sc(s)I	Sc	Sb
NGC 3949.....	SA(s)bc	Sc(s)II–III	SABbc	SABcd
NGC 4027.....	SB(s)dm	Sc(s)II.2	SBd	SBd
NGC 4030.....	SA(s)bc		Sb	Sab
NGC 4038.....	SB(s)m pec	Sc (tides)	S pec	S pec
NGC 4039.....	SA(s)m pec	Sc (tides)	S pec	S pec
NGC 4051.....	SAB(rs)bc	Sbc(r)II	SBbc	SBb
NGC 4062.....	SA(s)c	Sc(s)II–III	Sc	Sb
NGC 4100.....	(R′)SA(rs)bc	Sc(s)I–II	Sbc	SBbc
NGC 4123.....	SB(r)c	SBbc(rs)I.8	SBbc	SBb
NGC 4136.....	SAB(r)c	Sc(r)I–II	SAB(r)bc	SB(r)a
NGC 4145.....	SAB(rs)d	Sc(r)II	SAB(r)c	SBc
NGC 4151.....	(R′)SAB(rs)ab:	Sab	SBa	SB0/a
NGC 4178.....	SB(rs)dm	SBc	SBcd	SBc? (edge-on)
NGC 4212.....	SAc:	Sc(s)II–III	Sbc	SABbc
NGC 4242.....	SAB(s)dm	Sd/SBd	SBdm	SBm
NGC 4254.....	SA(s)c	Sc(s)I.3	Sc	SABc
NGC 4293.....	(R)SB(s)0/a	Sa	(R)Sab pec	SBab
NGC 4303.....	SAB(rs)bc	Sc(s)I.2	SBbc	SBbc
NGC 4314.....	SB(rs)a	SBa(rs) pec	(R)SB(r)0/a pec	(R)SBa
NGC 4388.....	SA(s)b: sp	Sab	Sab?	SB(r)a
NGC 4394.....	(R)SB(r)b	SBb(sr)I–II	SB(r)ab	(R)SB0/a
NGC 4414.....	SA(rs)c?	Sc(sr)II.2	Sbc	Sab
NGC 4448.....	SB(r)ab	Sa(late)	SAB(r)a	SB(r)a
NGC 4450.....	SA(s)ab	Sab pec	(R)Sa	SBab
NGC 4457.....	(R)SAB(s)0/a	RSb(s)II	(R)Sab	(R)SB0/a
NGC 4487.....	SAB(rs)cd	Sc(s)II.2	SABcd	SBd
NGC 4490.....	SB(s)d pec	Scd/SBcd	SBd	SBm
NGC 4496A.....	SB(rs)m		SB(r)d	SBd? pec
NGC 4504.....	SA(s)cd	Sc(s)II	Scd	SBcd
NGC 4527.....	SAB(s)bc	Sb(s)II	Sb	SABab
NGC 4548.....	SB(rs)b	SBb(rs)I–II	SB(r)ab	SBab
NGC 4568.....	SA(rs)bc	Sc(s)II–III	Sc pec	Sbc
NGC 4571.....	SA(r)d	Sc(s)II–III	S(r)c	Scd
NGC 4579.....	SAB(rs)b	Sab(s)II	SB(r)ab	SBa
NGC 4580.....	SAB(rs)a pec	Sc(s)/Sa	S(r)b	S(r)b
NGC 4593.....	(R)SB(rs)b	SBb(rs)I–II	SB(r)ab	SBa
NGC 4618.....	SB(rs)m	SBbc(rs)II.2	SBdm	SBm
NGC 4643.....	SB(rs)0/a	SB03/SBa	SB(r)0/a	SB0
NGC 4647.....	SAB(rs)c		SB(r)c	SBbc
NGC 4651.....	SA(rs)c	Sc(r)I–II	Sbc	SABa
NGC 4654.....	SAB(rs)cd	SBc(rs)II–III	SABbc	SBcd
NGC 4665.....	SB(s)0/a		SB0/a	(R)SBa

TABLE 1—*Continued*

Name (1)	RC3 Type (2)	CAG Type (3)	OSU *B* Type (4)	OSU *H* Type (5)
NGC 4666.....	SABc:	SBcII.3	Sbc?	SBc? (edge-on)
NGC 4689.....	SA(rs)bc	Sc(s)II.3	Sbc	Sb
NGC 4691.....	(R)SB(s)0/a pec	R Amorph pec	(R)SBd pec	SBd
NGC 4698.....	SA(s)ab	Sa	Sa	S(r)a
NGC 4699.....	SAB(rs)b	Sab(sr) or Sa	SBa	SB0
NGC 4772.....	SA(s)a		Sa	(R)SB0
NGC 4775.....	SA(s)d	Sc(s)III	Sd	Sd
NGC 4781.....	SB(rs)d	Sc(s)III	SABdm	SBdm
NGC 4818.....	SAB(rs)ab:		S pec	SB0/a
NGC 4856.....	SB(s)0/a	S01(6)/Sa	S0/a	S0/a
NGC 4900.....	SB(rs)c		SBd	SBdm
NGC 4902.....	SB(r)b	SBb(rs)I–II	SB(r)b	SB(r)b
NGC 4930.....	SB(rs)b		SB(r)b	SB(r)ab
NGC 4939.....	SA(s)bc	Sbc(rs)I	SABb	SABb
NGC 4941.....	(R)SAB(r)ab:	Sab(s)II	SABab	SABa
IC 4182	SA(s)m		Sm	dI
NGC 4995.....	SAB(rs)b	Sbc(s)II	SAB(r)ab	SBab
NGC 5005.....	SAB(rs)bc	Sb(s)II	Sb	SBa
NGC 5054.....	SA(s)bc	Sb(s)I–II	Sc	SABc
NGC 5078.....	SA(s)a: sp		Sa?	Sa (edge-on)
NGC 5085.....	SA(s)c	Sc(r)II	Sc	SABbc
NGC 5101.....	(R)SB(rs)0/a	SBa	(R)SB(r)0/a	(R)SB0/a
NGC 5121.....	(R′)SA(s)a	Sa	S0/a	S0
NGC 5161.....	SA(s)c:	Sc(s)I	Sc	SBab
NGC 5247.....	SA(s)bc	Sc(s)I–II	Sc	Sc
NGC 5248.....	SAB(rs)bc	Sbc(s)I–II	S(r)c	Sb
ESO 383-G87.....	SB(s)dm		SBm	dI
NGC 5334.....	SB(rs)c:	SBc(rs)II	SBcd	SBd
NGC 5371.....	SAB(rs)bc	Sb(rs)I/SBb(rs)I	SABbc	SBbc
NGC 5427.....	SA(s)c pec	Sbc(s)I	S(r)c	Sc
NGC 5448.....	(R)SAB(r)a	Sa(s)	SAB(r)b	SABa
NGC 5483.....	SA(s)c	SBbc(s)II–III	SABc	SBc
NGC 5530.....	SA(rs)c	Sc(s)II.8		
IC 4402	SA(s)b? sp		Scd?	Sc? (edge-on)
IC 4444	SAB(rs)bc:	Sc(s)II pec	Sd	(R)SB(r)cd
NGC 5643.....	SAB(rs)c	SBc(s)II–III	SAB(r)b	SB(r)a
NGC 5676.....	SA(rs)bc	Sc(s)II	Sbc	SABbc
NGC 5701.....	(R)SB(rs)0/a	(PR)SBa	(R)SB0/a	(R)SB0
NGC 5713.....	SAB(rs)bc pec	Sbc(s) pec	SABd	SBdm
NGC 5850.....	SB(r)b	SBb(sr)I–II	SB(r)ab	SB(r)0/a
NGC 5921.....	SB(r)bc	SBbc(s)I–II	SB(r)bc	SB(r)bc
NGC 5962.....	SA(r)c	Sc(rs)II.3	SABb	SBab
NGC 6215.....	SA(s)c	Sc(s)II	Scd	SABbc
NGC 6221.....	SB(s)c	Sbc(s)II–III	SABcd	SBb
ESO 138-G10.....	SA(s)dm		Sdm	S0
NGC 6300.....	SB(rs)b	SBb(s)II pec	SAB(r)bc	SB(r)a
NGC 6384.....	SAB(r)bc	Sb(r)I.2	SB(r)bc	SBbc
NGC 6753.....	(R′)SA(r)b	Sb(r)I	(R)S(r)a	Sa
NGC 6782.....	(R)SAB(r)a	SBab(s)	(R)SAB(r)a	(R)SB0/a
ESO 142-G19.....	Sb: sp		Sa? (edge-on)	Sa? (edge-on)
NGC 6902.....	SA(r)b	Sa(r)	S(r)ab	SB(r)a
NGC 6907.....	SB(s)bc	SBbc(s)II	SBc	SBbc
IC 5052	SBd: sp	Scd/SBcd	Sd?	Sd
NGC 7083.....	SA(s)bc	Sb(s)I–II	Sbc	Sb
NGC 7184.....	SB(r)c	Sb(r)II	S(r)a?	SB(r)a
NGC 7205.....	SA(s)bc	Sb(r)II.8	Sb	SABb
NGC 7213.....	SA(s)a:	Sa(rs)	Sa	S0
NGC 7217.....	(R)SA(r)ab	Sb(r)II–III	(R)Sa	S0/a
NGC 7314.....	SAB(rs)bc	Sc(s)III		
NGC 7410.....	SB(s)a	SBa or Sa		
NGC 7412.....	SB(s)b	Sc(s)I–II	SABc	SABc
NGC 7418.....	SAB(rs)cd	Sc(rs)I.8	SABbc	SBbc
IC 5267	(R)SA(rs)0/a	Sa(r)		
IC 5271	Sb?	Sb(rs)II		
IC 5273	SB(rs)cd	SBc(s)II–III		

TABLE 1—*Continued*

Name (1)	RC3 Type (2)	CAG Type (3)	OSU *B* Type (4)	OSU *H* Type (5)
NGC 7479.....	SB(s)c	SBbc(s)I–II	SBbc	(R)SBbc
NGC 7496.....	(R′:)SB(rs)bc	SBc(s)II.8		
NGC 7513.....	(R′)SB(s)b pec			
NGC 7552.....	(R′)SB(s)ab	SBb(s)I–II	(R)SBb	(R)SBa
NGC 7582.....	(R_1')SB(s)ab	SBab(rs)	SBb?	(R)SBb? (edge-on)
NGC 7606.....	SA(s)b	Sb(r)I	Sab	Sab
IC 5325	SAB(rs)bc	Sc(s)II–III	Sbc	SABbc
NGC 7713.....	SB(r)d:	Sc(s)II–III	Sd	Sdm
NGC 7723.....	SB(r)b	SBb(rs)I–II	SB(r)bc	SB(r)ab
NGC 7727.....	SAB(s)a pec	Sa pec	SABa pec	S pec (early)
NGC 7741.....	SB(s)cd	SBc(s)II.2	SBcd	SBcd
NGC 7814.....	SA(s)ab: sp	S(ab)	Sa? (edge-on)	S0/a (edge-on)

classification to earlier types. Structures that are dominated by either younger stellar populations or absorption effects will be less prominent in the near-IR than the optical. Flocculent spiral features, dominated either by OB stars or by dust lanes, may disappear in the near-IR, again leading to earlier morphological classification. Also features such as resonance rings that are currently lit up by star formation may be less prominent or unseen in the near-IR (see the images of NGC 6782 on the Survey Web page for an example). Grand-design spiral patterns are seen in near-IR imaging of many spirals (e.g., Puerari et al. 2000); thus, spiral patterns are not traced out by only the young stars. In fact, there is evidence from the study of a small sample that there can be drastic differences in the pitch angle of the spiral pattern measured in the optical and the near-IR (Block & Puerari 1999). The assertion of Block & Puerari (1999) that the optical and near-IR morphologies of spiral galaxies are uncorrelated begs for a comparative study of the optical and near-IR morphological types of a large unbiased sample of spirals such as ours.

One of us (P. B. E.) classified the entire sample in both *B* and *H* twice, with excellent overall agreement between the trials in each waveband: more than 80% of the classifications agreed to within two subtypes (i.e., Sa to Sb). We also cross-checked our results by comparing classifications done by two of us (P. B. E. and J. A. F.). We selected 40 galaxies from the sample in *B*, and 40 in *H* and compared our classifications for these subsets. For both the *B*- and *H*-band subsets, more than 80% of the tested galaxies were assigned types that again agreed to within two subtypes. In no case were there any systematic differences between any of our sets of classifications. This compares well with the scatter between classifiers reported by Naim et al. (1995). Figure 2 shows comparisons of classifications, parameterized as T types, following the RC3. We compare the optical classifications of the RC3 and the CAG to one another, and both of these catalog classifications with our optical and near-IR classifications. Tables 2A–2F give the average and median differences and dispersions as a function of Hubble type for each of the classification pairs shown in Figure 2. We note that we are presently interested in Hubble stage and bar family classification only. Although we note the presence of inner (r) and outer (R) ring structures when they are obvious, we otherwise feel unqualified to make variety classifications (rs and s types) as defined by de Vaucouleurs (1959) or detailed ring morphology classifications as defined by Buta (1986, 1995).

Figure 2*a* and Table 2A show a good agreement between the RC3 and the CAG for types Sab through Sc ($2 \leq T \leq 5$). For galaxies with RC3 types S0/a and Sa, the CAG gives slightly later classifications. It is well known that the CAG classifies very few galaxies as later than Sc; thus, the disagreement with the RC3 at late types is expected. Figure 2*b* and Table 2B show our OSU *B*-band types against the RC3 types. Overall, the agreement is excellent. We tend to classify galaxies with RC3 types S0/a and Sa ($0 \leq T \leq 1$) as having marginally later type and galaxies with RC3 types later than Sc ($T > 5$) as having marginally earlier types. However, our optical classifications agree with the RC3 to within the dispersion for all types S0/a through Sm. In Figure 2*c* and Table 2C we compare our *B*-band types with the CAG. For galaxies with CAG types of S0/a through Sc ($0 \leq T \leq 5$) our optical types match even better than with the RC3. The disagreement at later types is consistent with what is seen in Figure 2*a*.

In Figure 2*d* and Table 2D, we compare our *H*-band types with the RC3 types. For the earliest (S0/a and Sa, or $0 \leq T \leq 1$) and latest (Scd through Sm, or $6 \leq T \leq 9$) types, the agreement is excellent. But for galaxies with RC3 types from Sab through Sc ($2 \leq T \leq 5$), our *H*-band types are roughly one subclass earlier than the RC3 types on average. While this is within the dispersion for any given type, the effect is persistent across the range of mid-type spirals. We compare our *H*-band types with the CAG in Figure 2*e* and Table 2E. Our *H*-band classifications are earlier on average by about one subclass from CAG types S0/a through Sbc ($0 \leq T \leq 4$). At Sc ($T = 5$), we are in rough agreement, and there are too few galaxies with CAG types later than Sc for any meaningful comparison. Finally, in Figure 2*f* and Table 2F, we compare our *B*-band classifications with our *H*-band classifications. For all OSU Survey *B*-band types Sa through Scd ($1 \leq T \leq 6$), we assign *H*-band types that are roughly one subclass earlier than the optical types. At the very earliest (S0/a) and latest (Sd through Sm) types, our *B*-band classifications agree with our *H*-band classifications on average.

In summary, we find that spiral galaxies with optical classifications of roughly Sab through Sc ($2 \leq T \leq 5$) appear about one T type earlier in the *H* band on average. This result persists for all optical classifications (RC3, CAG, and our own). And the disagreement between optical and near-

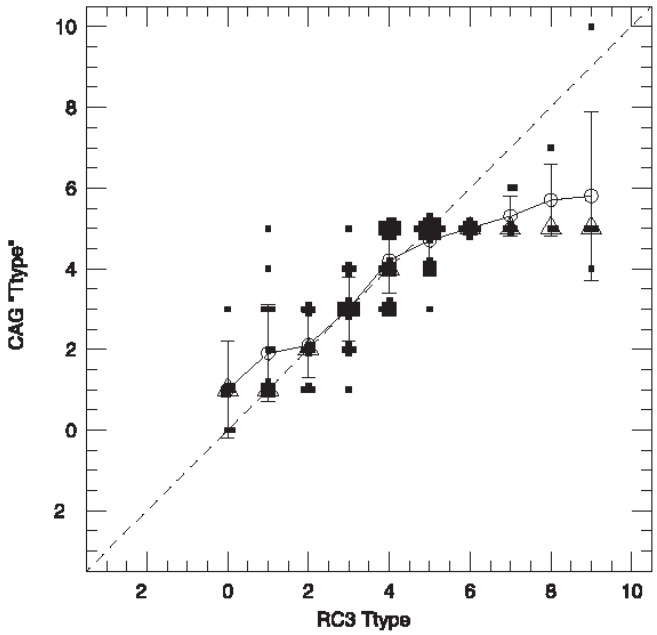


FIG. 2*a*

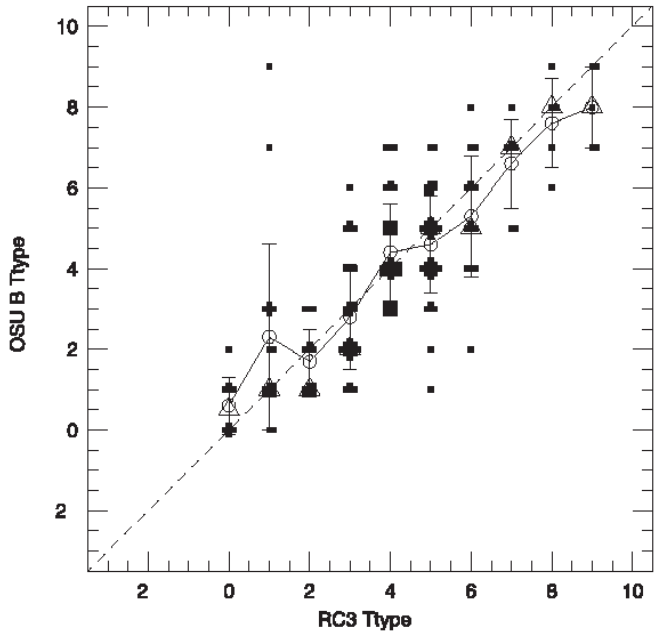


FIG. 2*b*

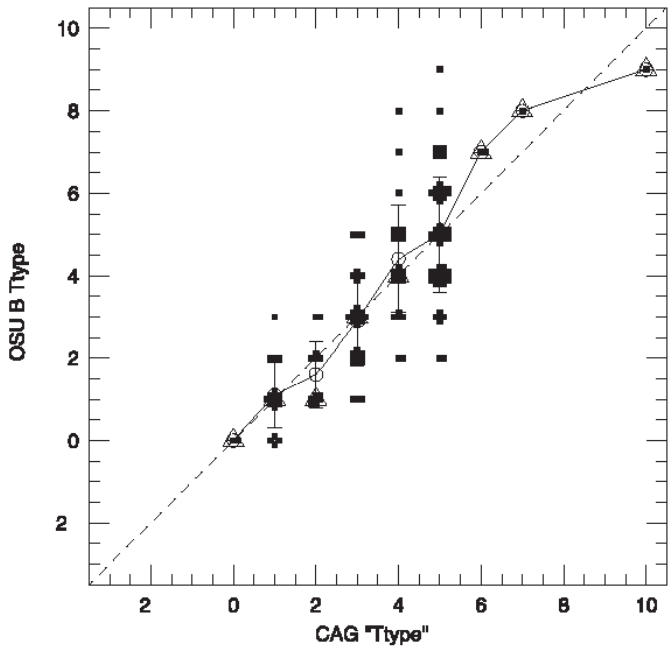


FIG. 2*c*

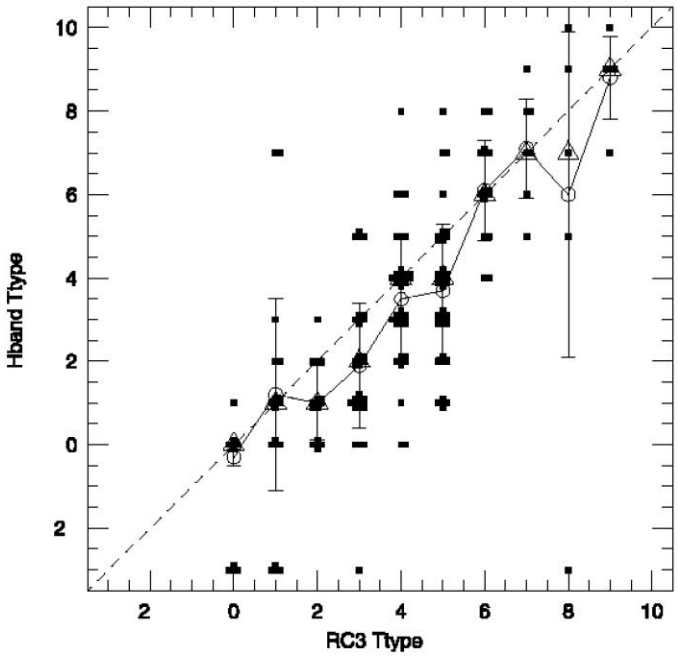


FIG. 2*d*

FIG. 2.—Comparisons of morphological types from the RC3, the CAG, our *B*-band data, and our *H*-band data. (*a*) RC3 types vs. CAG types, (*b*) RC3 types vs. OSU *B*-band types, (*c*) CAG types vs. OSU *B*-band types, (*d*) RC3 types vs. OSU *H*-band types, (*e*) CAG types vs. OSU *H*-band types, (*f*) OSU *B*-band types vs. OSU *H*-band types. The size of the solid polygons scale with the number of galaxies at that location. The open circles are the mean *y*-axis values for a given *x*-axis value, and the error bars are the dispersions about those means. The large open triangles are the median *y*-axis values for a given *x*-axis value. For statistical purposes, objects classified as S0 are scored as $T = -1$.

IR classes occurs in the range of morphological types over which all optical classifications are in good agreement. For the earliest (S0/a and Sa) and latest (Scd through Sm) types, there is no wavelength dependence in the morphological classification. While there have been a number of studies comparing galaxy morphology in the optical and near-IR (see § 1), these have mainly been studies of individual galaxies or at most small samples. Ours is the first result showing the nature of the morphological *K*-correction (the change in morphology as a function of observed rest wavelength) for a large, statistically complete sample of spirals. Thus, it is worth considering possible physical reasons for our results.

For the earliest types (S0/a and Sa), there is no disagreement in the mean between the optical and near-IR classifications. As these galaxies have very little ongoing star formation, and very little dust, both the optical and near-IR morphologies are dominated by the distribution of old, late-

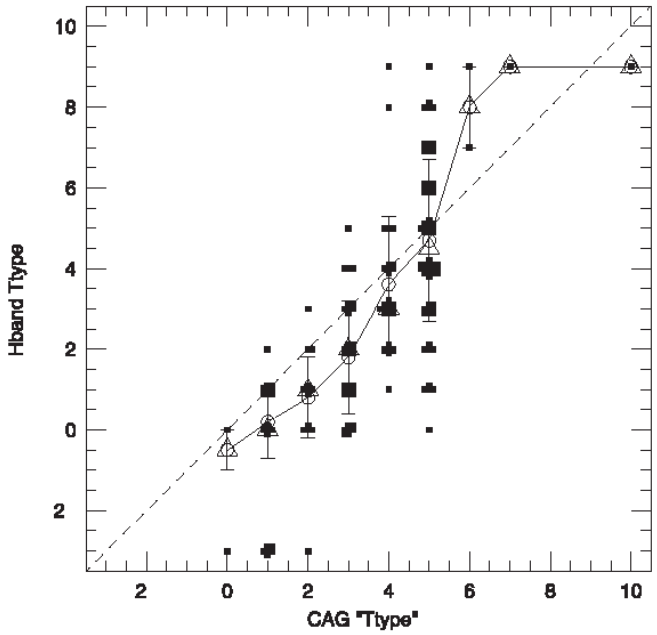


FIG. 2*e*

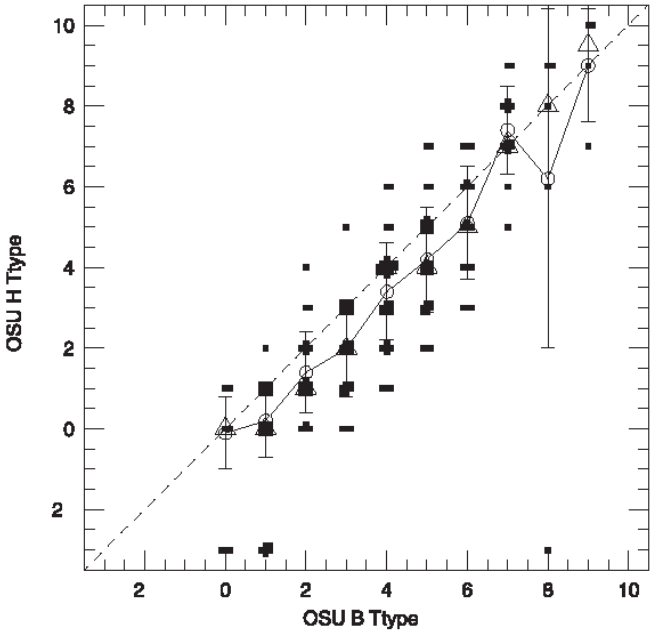


FIG. 2*f*

type stars. The two wavebands should give similar classifications, and we are reassured that they, in fact, do so.

We find an average disagreement of one subclass between the optical and near-IR classifications of mid-type spirals (optical classifications Sab through Sc), in the sense that the near-IR classifications tend to be earlier than the optical classifications. As noted above, bulges are more prominent and spiral arms are less knotty in the near-IR than in the optical. This drives the earlier classification of mid-type spirals in the near-IR.

We see no disagreement in the mean for the latest type galaxies (Scd through Sm). These are galaxies that are dominated by ongoing star formation, so this seems surprising at first. However, very late-type galaxies have poorly defined

TABLE 2A

COMPARISON BETWEEN THE RC3 AND CAG

RC3 Type	Number	Mean CAG Type	(RC3−CAG)	Dispersion	Median
0.....	10	1.0	−1.0	1.2	1
1.....	17	1.9	−0.9	1.2	1
2.....	15	2.1	−0.1	0.8	2
3.....	29	3.0	0.0	0.8	3
4.....	42	4.2	−0.2	0.8	4
5.....	40	4.7	0.3	0.5	5
6.....	14	5.0	1.0	0	5
7.....	7	5.3	1.5	0.5	5
8.....	3	5.7	2.3	0.9	5
9.....	5	5.8	3.2	2.1	5

TABLE 2B

COMPARISON BETWEEN THE RC3 AND OSU *B*

RC3 Type	Number	Mean OSU *B* Type	(RC3−OSU *B*)	Dispersion	Median
0.....	10	0.6	−0.6	0.7	0.5
1.....	19	2.3	−1.3	2.3	1
2.....	15	1.7	0.3	0.8	1
3.....	32	2.8	0.2	1.3	2
4.....	41	4.4	−0.4	1.2	4
5.....	41	4.6	0.4	1.2	5
6.....	15	5.3	0.7	1.5	5
7.....	7	6.6	0.4	1.1	7
8.....	5	7.6	0.4	1.1	8
9.....	5	8.0	1.0	1.0	8

TABLE 2C

COMPARISON BETWEEN THE CAG AND OSU *B*

CAG Type	Number	Mean OSU *B* Type	(CAG−OSU *B*)	Dispersion	Median
0.....	2	0	0	0	0
1.....	20	1.1	−0.1	0.8	1
2.....	13	1.6	0.4	0.8	1
3.....	34	2.9	0.1	1.1	3
4.....	28	4.4	−0.4	1.3	4
5.....	68	5.0	0	1.4	5
6.....	2	7.0	−1.0	0	7
7.....	1	8.0	−1.0	0	8
10.....	1	9.0	1.0	0	9

TABLE 2D

COMPARISON BETWEEN THE RC3 AND OSU *H*

RC3 Type	Number	Mean OSU *H* Type	(RC3−OSU *H*)	Dispersion	Median
0.....	10	−0.3	0.3	0.2	0
1.....	18	1.2	−0.2	2.3	1
2.....	16	1.0	1.0	0.9	1
3.....	32	1.9	1.1	1.5	2
4.....	41	3.5	0.5	1.5	4
5.....	41	3.7	1.3	1.6	4
6.....	16	6.1	−0.1	1.2	6
7.....	7	7.1	−0.1	1.2	7
8.....	5	6.0	2.0	3.9	7
9.....	5	8.8	0.2	1.0	9

TABLE 2E

COMPARISON BETWEEN THE CAG AND OSU *H*

CAG Type	Number	Mean OSU *H* Type	(CAG−OSU *H*)	Dispersion	Median
0.....	2	−0.5	0.5	0.5	−0.5
1.....	20	0.2	0.8	0.9	0
2.....	13	0.8	1.2	1.0	1
3.....	34	1.8	1.2	1.4	2
4.....	28	3.6	0.4	1.7	3
5.....	68	4.7	0.3	2.0	4.5
6.....	2	8.0	−2.0	1.0	8
7.....	1	9.0	−2.0	0	9
10.....	1	9.0	1.0	0	9

TABLE 2F

COMPARISON BETWEEN THE OSU *B* AND OSU *H*

OSU *B* Type	Number	Mean OSU *H* Type	(OSU *B*−OSU *H*)	Dispersion	Median
0.....	7	−0.1	0.1	0.9	0
1.....	25	0.2	0.8	0.9	0
2.....	22	1.4	0.6	1.0	1
3.....	28	2.0	1.0	1.2	2
4.....	35	3.4	0.6	1.2	4
5.....	32	4.2	0.8	1.3	4
6.....	17	5.1	0.9	1.4	5
7.....	15	7.4	−0.4	1.1	7
8.....	5	6.2	1.8	4.2	8
9.....	4	9.0	0	1.4	9.5

spiral structure and very weak or nonexistent bulges as matters of definition. The things that work to drive the sort of morphological *K*-correction we see for the mid-type spirals are the relative prevalence of the bulge and the difference in contrast and appearance of spiral arms traced by sites of ongoing star formation (in the optical) or by the distribution of old, late-type giants (in the near-IR). Galaxies with no bulge and very poorly defined spiral patterns will not look substantially different in the near-IR than in the optical and will thus be classified essentially the same on average.

4. NOTES ON INDIVIDUAL GALAXIES

Below, we provide brief descriptions of the *H*-band morphology of each survey galaxy, along with our *H*-band morphological classifications. For galaxies with OSU Survey *B* types more than two subtypes different (later in all cases) than their OSU Survey *H* types, we discuss the features that drive the earlier classification in the *H* band. Table 3 gives a set of *H*-band type examples for each morphological class. We show *B*- and *H*-band images of these type examples in Figure 3. The images in Figure 3 are typically shown in an 8 bit logarithmic stretch with white set at 2 σ below the sky level and black at the peak value. We adjusted this in cases with bright nuclear sources. In Figure 4, we show color-composite images (blue is *B*, green is *R*, red is *H*) of six galaxies. We selected two early-type, two mid-type, and two late-type spirals to show in Figure 4. Within each pair, we selected one object that is given the same classification in the optical and near-IR and one that is classified at least a full Hubble type earlier in the near-IR than in the *B* band.

NGC 150.—SBb: Strong bar. Two-arm grand-design spiral. Asymmetric arms that start before the intersection point with the bar. Regions of strong star formation in the areas near the arm-bar contacts. SE arm bifurcates just beyond the bar contact point. NW arm is more linear than the SE arm.

NGC 157.—Sbc (type example—see Fig. 3*f*): No apparent bar. Grand-design spiral pattern. Oval bulge with the arms beginning at the ends of the bulge *minor* axis. SW arm initially linear, then begins to wind, and bifurcate as it crosses the disk major axis. Arm fades after only 180°. NE arm is very wide to NE and appears to wrap a full turn before it fades away. The optical types for this galaxy are SAB(rs)bc: (RC3), Sc(s)II–III (CAG), and SBbc (OSU *B*). It is thus a rare example of a galaxy that appears optically barred, but unbarred in the near-IR. What appears to be a bar in the optical looks much more like the result of projection in the near-IR.

NGC 210.—(R)SB0/a: Strong bulge threaded by thick, high-contrast bar with visible ansae at the ends. Faint outer ring (not obviously a spiral pattern) with star-forming knots.

NGC 278.—Sb: Face-on. Centrally condensed, resolved circular nucleus, embedded in a slightly elliptical bulge. Fairly high B/D ratio. Two-armed spiral pattern, with tightly wrapped spiral arms. Arms have obvious dust lanes and numerous bright star-forming knots.

NGC 289.—SB(r)ab (type example—see Fig. 3*d*): Strong bar and aligned elliptical bulge. Symmetric two-arm pattern emerges from the ends of the bar. Arms are smooth and well-defined. Arms both bifurcate after ~90°. Log stretch shows bright ansae at the ends of the bar.

NGC 428.—SBm (type example—see Fig. 3*k*): Nuclear point source embedded in an asymmetric inner disk. No true bulge. Outer disk has numerous star-forming knots, and evidence for two very asymmetric spiral arms. The NW arm is fairly tightly wrapped, and the better defined of the two in its inner part. It has several very bright knots through ~60° of winding to the east. It then becomes very diffuse and poorly defined but can still be traced as a low surface brightness (LSB) feature through a winding angle of ~180°. The SE arm is very loosely wrapped and has LSB. It can be followed for ~100° to the west.

NGC 488.—Sa (type example—see Fig. 3*c*): System nearly face-on. Bright, circular nucleus, embedded in a large, slightly elliptical bulge. The bulge and disk have the same P.A. There is a faint spiral pattern, with thin, smooth tightly wrapped arm features embedded in a smooth disk. There are no prominent star-forming knots.

NGC 578.—SBc: Very small, slightly elliptical bulge, with prominent bar running E–W. System at fairly high inclination. Arms originate at ends of bar, at very steep angles (closer to 120° than 90°). Arms well-defined for almost 180°, then they break up. SE arm bifurcates. NW arm becomes very diffuse. A few knots in the inner arms. Outer arms are very lumpy. A bright companion is just to the east, superposed on one bifurcation of the SE arm.

NGC 613.—SB(r)bc (type example—see Fig. 3*f*): Bright nuclear point source. Nuclear bar aligned with elliptical bulge and large normal bar. Fairly highly inclined disk. Two

TABLE 3
H-BAND TYPE EXAMPLES

OSU *H* Type	SA	SAB	SB	Fig. 3
S0	NGC 7213		NGC 1317	*a*
S0/a	NGC 7217	NGC 1617	NGC 5850	*b*
Sa	NGC 488	NGC 1371	NGC 1350	*c*
Sab	NGC 7606	NGC 3705	NGC 289	*d*
Sb	NGC 2090	NGC 7205	NGC 1300	*e*
Sbc	NGC 157	IC 5325	NGC 613	*f*
Sc	NGC 5247	NGC 7412	NGC 4145	*g*
Scd	NGC 4571	NGC 3949	NGC 685	*h*
Sd	NGC 3423		NGC 4027	*i*
Sdm	NGC 7713		NGC 1385	*j*
Sm	NGC 625		NGC 428	*k*
dI	ESO 383-G87			*k*

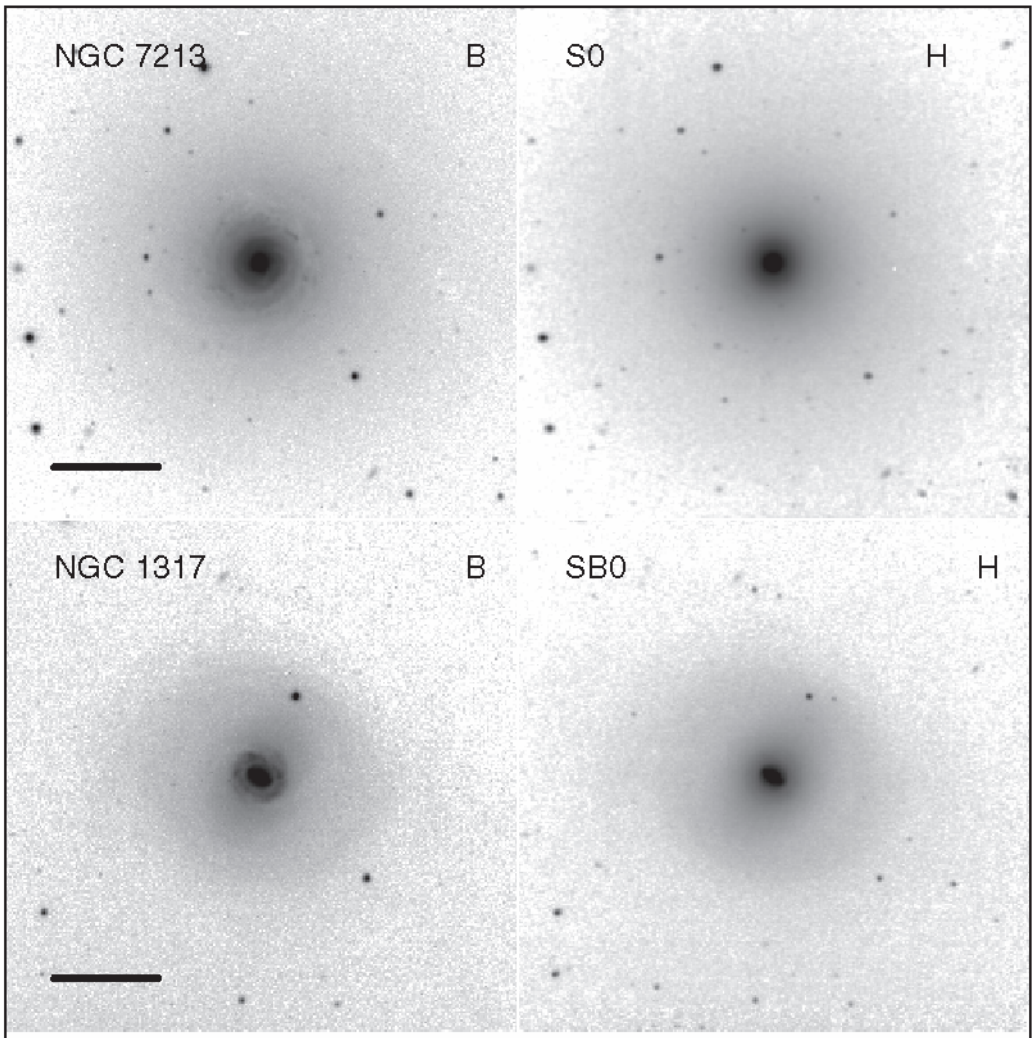


FIG. 3*a*

FIG. 3.—*B*- and *H*-band images of galaxies selected as *H*-band type examples. The *B* images are on the left, and the *H* images are on the right. All images are oriented N up, E to the left. The scale bars on the *B* images are 1′ long; each *BH* image pair are at the same scale. The OSU *H*-band types are shown on the *H*-band images. (*a*) NGC 7213—S0 (*top*) and NGC 1317—SB0 (*bottom*). (*b*) NGC 7217—S0/a (*top*); NGC 1617—SAB0/a (*middle*); NGC 5850—SB0/a (*bottom*). (*c*) NGC 488—Sa (*top*); NGC 1371—SABa (*middle*); NGC 1350—SBa (*bottom*). (*d*) NGC 7606—Sab (*top*); NGC 3705—SABab (*middle*); NGC 289—SBab (*bottom*). (*e*) NGC 2090—Sb (*top*); NGC 7205—SABb (*middle*); NGC 1300 SBb (*bottom*). (*f*) NGC 157—Sbc (*top*); IC 5325—SABbc (*middle*); NGC 613—SBbc (*bottom*). (*g*) NGC 5247—Sc (*top*); NGC 7412—SABc (*middle*); NGC 4145—SBc (*bottom*). (*h*) NGC 4571—Scd (*top*); NGC 3949—SABcd (*middle*); NGC 685—SBcd (*bottom*). (*i*) NGC 3423—Sd (*top*); NGC 4027—SBd (*bottom*). (*j*) NGC 7713—Sdm (*top*); NGC 1385—SBdm (*bottom*). (*k*) NGC 625—Sm (*top*); NGC 428—SBm (*middle*); ESO 383-G87—dI (*bottom*).

bright arms emerge from the ends of the bar, with many bright knots near the bar ends. SE arm wraps loosely to the NE. NW arm wraps tightly to the SW and forms an inner disk ring. Several other, lower surface brightness arms emerge from the ring.

NGC 625.—Sm (type example—see Fig. 3*k*): No central concentration. Thick disk, seen close to edge-on. No evidence of spiral structure. System is rich in star-forming knots/bright star clusters.

NGC 685.—SBcd (type example—see Fig. 3*h*): Bright elongated nucleus, extending into a thin bar. Patchy, LSB arms emerge perpendicular to the bar ends. Arms fade out after $\sim 270^{\circ}$.

NGC 779.—SAB(r)b: Bright nucleus embedded in an elliptical/boxy bulge. System has high inclination. Grand-design two-armed spiral pattern, with the arms emerging from the corners of the boxy bulge. The inner arms are high surface brightness (HSB) and form an inner pseudoring, with bright enhancements along the major axis. The arms are embedded in a smooth disk, with no pronounced star-forming knots. The break in the pseudoring to the NW side of the nucleus may be due to dust extinction. At lower surface brightness levels, the system is smooth and extends to very large radii.

NGC 864.—SBb: Strong, slightly curved bar, with bright ansae at the ends. Asymmetric arms that start before the intersection point with the bar. SE arm has a kinky appearance; more like a series of line segments than a smooth curve. Arms make less than a half-turn before losing their integrity. Outer spiral pattern is flocculent.

NGC 908.—Sc: Bright elliptical bulge, no evidence of a bar. Three-arm spiral pattern, with east arm much more open than north and SW arms. May be an inner ring in the disk. East arm bifurcates soon after it originates from a possible inner ring. SW arm is also peculiar. It emerges from the inner disk on the west side, curves to the south, and recon-

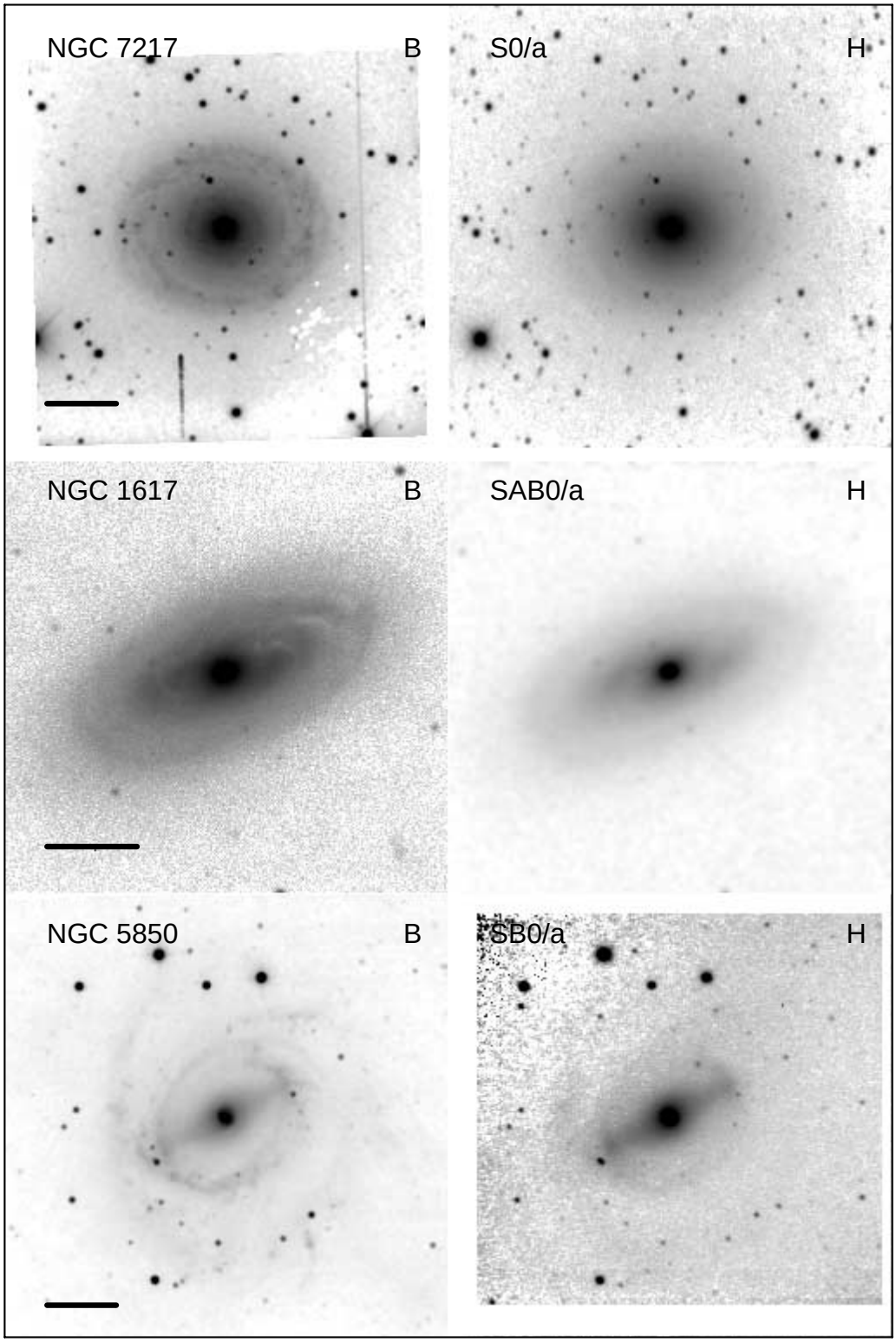


FIG. 3*b*

necks with the inner disk near the origin point of the east arm. Arms are patchy, with many obvious star-forming knots.

NGC 986.—No *JHK* data.

NGC 988.—SBcd: System close to edge-on. Nuclear point source embedded in a thin, slightly asymmetric bar. Inner bar is HSB. Outer bar is much lower surface brightness. Two thick, knotty, diffuse, filamentary spiral arms begin at the ends of the LSB bar and wrap for at least 180°. A bright star is superposed on the NW side of the disk.

IC 239.—SBc: System nearly face-on. Small circular bulge embedded in a thick bar. Disk is very LSB, with smooth two-armed grand-design spiral pattern. Arms seem

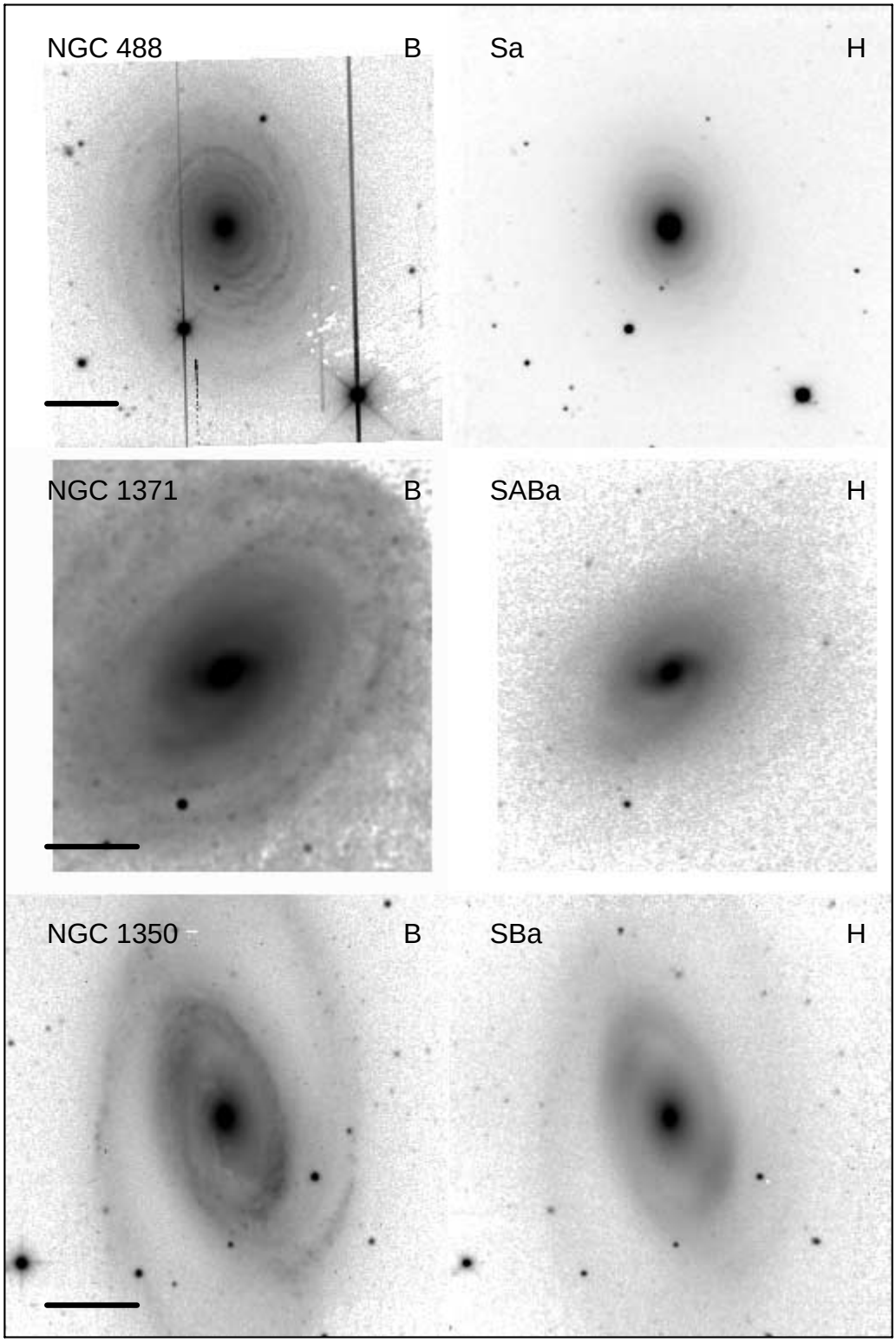


FIG. 3*c*

to begin from the long end of the bar (they are very fat at their base) and wind through ~180° before fading. LSB nature of the arms makes any internal structure hard to distinguish.

NGC 1003.—Scd?: Nearly edge-on. Weak nuclear point source embedded in a very flattened bulge/lens. Inner part of LSB disk has same P.A. as bulge/lens feature. At larger radii there is an obvious isophotal twist/warp. There are traces of a flocculent spiral pattern, and several knots of star formation.

NGC 1042.—SABc: Weak bar. Nuclear point source extends into mildly elliptical bulge. Classic two-armed spiral. Arm emerging from the NW side of the bulge has an HSB inner portion, becomes diffuse after ~30°, and

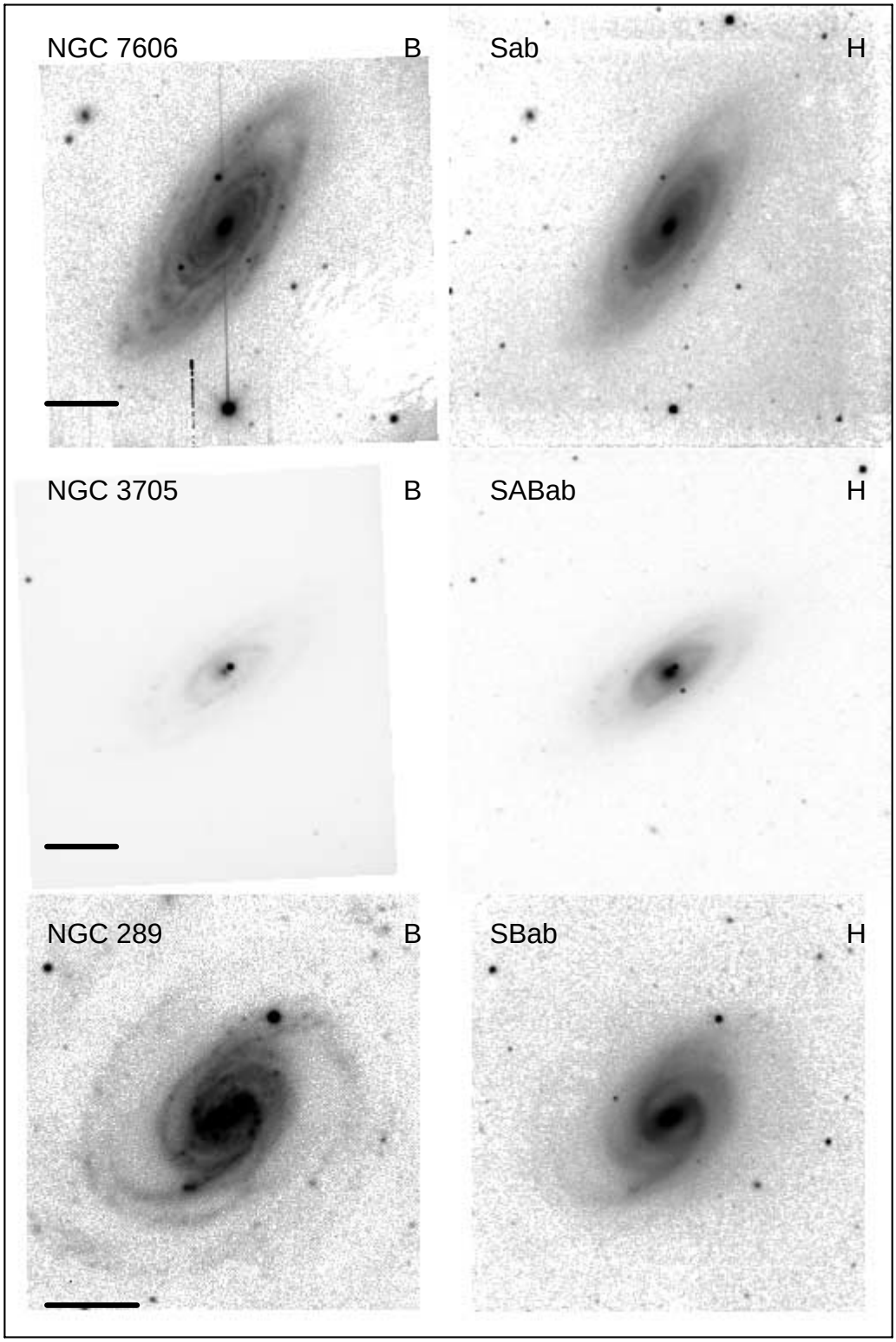


FIG. 3*d*

then becomes well defined again after $\sim 180^\circ$. There are a number of bright star-forming knots in the outer part of this arm. The NW arm winds through a total of $\sim 270^\circ$ before fading. SE arm is more regular, with an inner HSB region fading into an outer LSB region and not rebrightening. This arm can also be traced through $\sim 270^\circ$ before fading.

NGC 1058.—Sa: System close to face-on. Centrally peaked nuclear source. Clear break in surface brightness between the inner and outer disk. Very faint, flocculent irregular spiral pattern, with tightly wound arm segments.

NGC 1073.—SB(r)ab: Strong, thin bar, and very elliptical bulge. Weak grand-design arms form an inner ring. Arms originate at the ends of the bar and are roughly at right

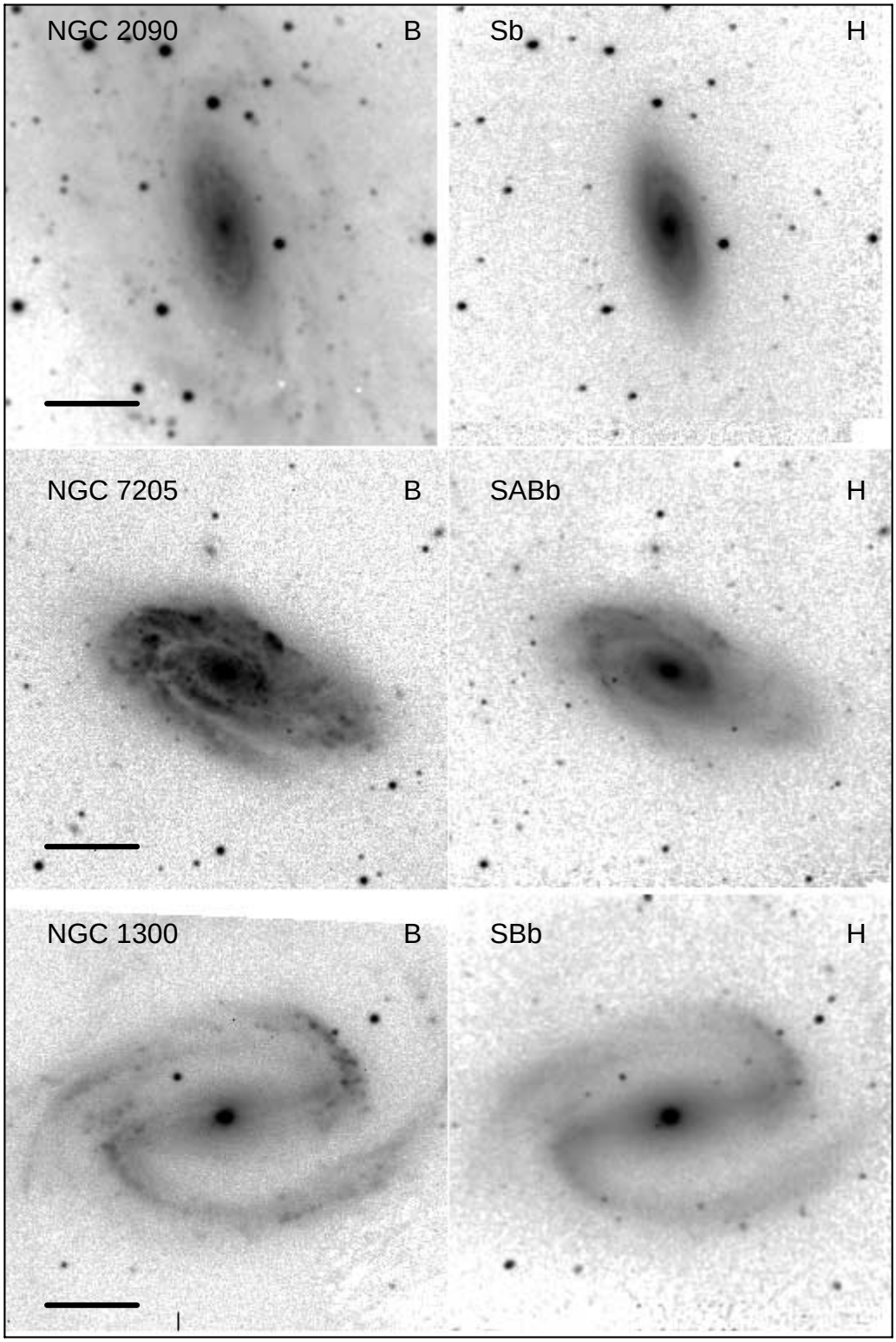


FIG. 3*e*

angles to the bar. The *B*-band type is SBc for all classifiers. We classify NGC 1073 substantially earlier in the *H* band because the outer, open spiral arms are very faint in the near-IR, leaving the inner arm/ring structure as the spiral feature that dominates the classification.

NGC 1084.—Sb: Bright nuclear point source. Bulge elongated along disk major axis; no sign of a bar. Multiarm pattern, but arms not very well defined. Inner arms have a number of bright knots. Arms wind about 180° before fading from view.

NGC 1087.—SBd: Face-on system with a small nuclear bar, and no true bulge. Bar is embedded in a knotty LSB disk, with wisps of spiral structure. At LSB, there is evidence for two very fat, open spiral features.

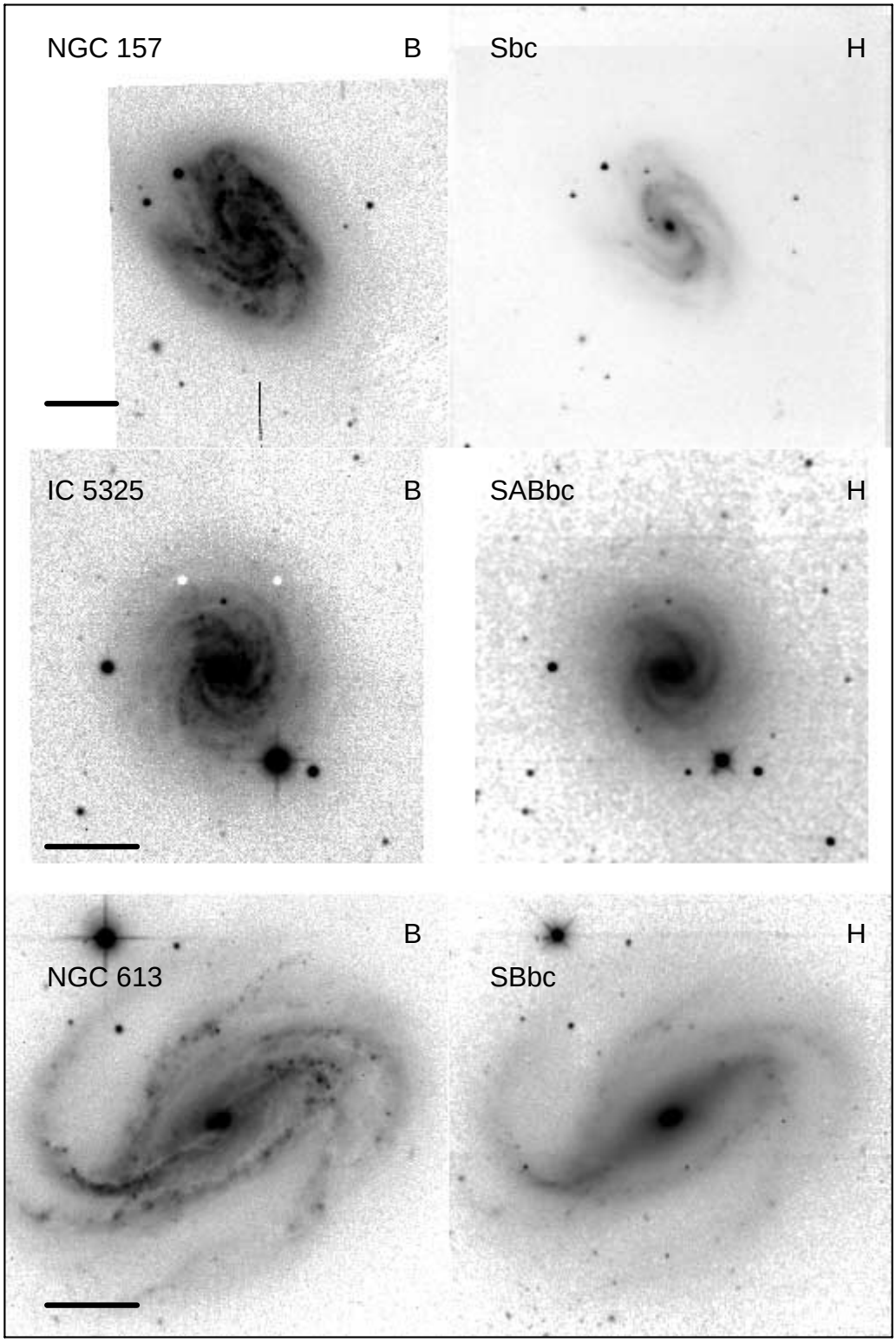


FIG. 3*f*

NGC 1187.—SB(r)b: Strong bar emerging along the major axis of an elliptical bulge (with nuclear point source). Spiral arms emerge from the ends of the bar. Arm beginning in the SE (and turning to the west) is fairly regular. Arm beginning at the NW end of the bar begins heading N, then fades out, and reappears to the east, heading SE. Arms have a few bright knots.

NGC 1241.—SB(r)ab: Nuclear point source. Bulge becomes elliptical/boxy at lower intensity levels. Prominent bar emerges from opposite corners of the boxy bulge. Strong two-arm pattern with arms originating in bright ansae at the ends of the bar. North arm is much more tightly wrapped than south arm. Several other arms appear at low surface brightness levels. LSB

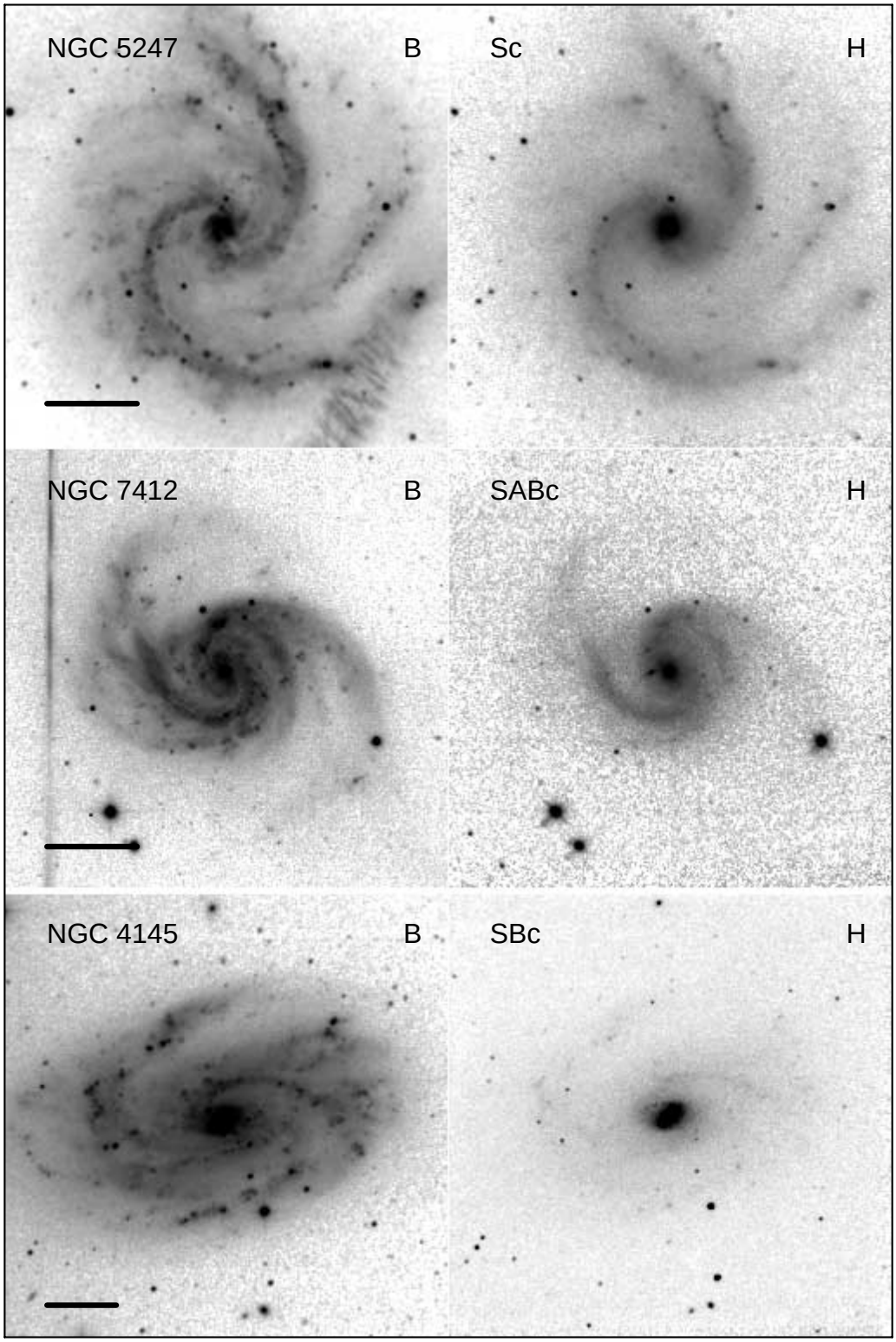


FIG. 3*g*

disk extends farther to the NW than the SE (disk major axis runs SE-NW). This may be due to an interaction with a fainter peculiar late-type galaxy to the NE.

NGC 1255.—No *JHK* data.

NGC 1300.—SBb (type example—see Fig. 3*e*): Strong bar, aligned with bulge major axis. Arms commence at the ends of the bar and are roughly perpendicular to the bar. Arms extend roughly 180° before fading. Far ends of the arms straighten out, rather than curving back into a pseudoring. Arms rich with star-forming knots.

NGC 1302.—SB0: Bright circular bulge, with a weak roughly N-S bar. Smooth lens outside bar. Perhaps a faint outer ring. No evidence for spiral structure.

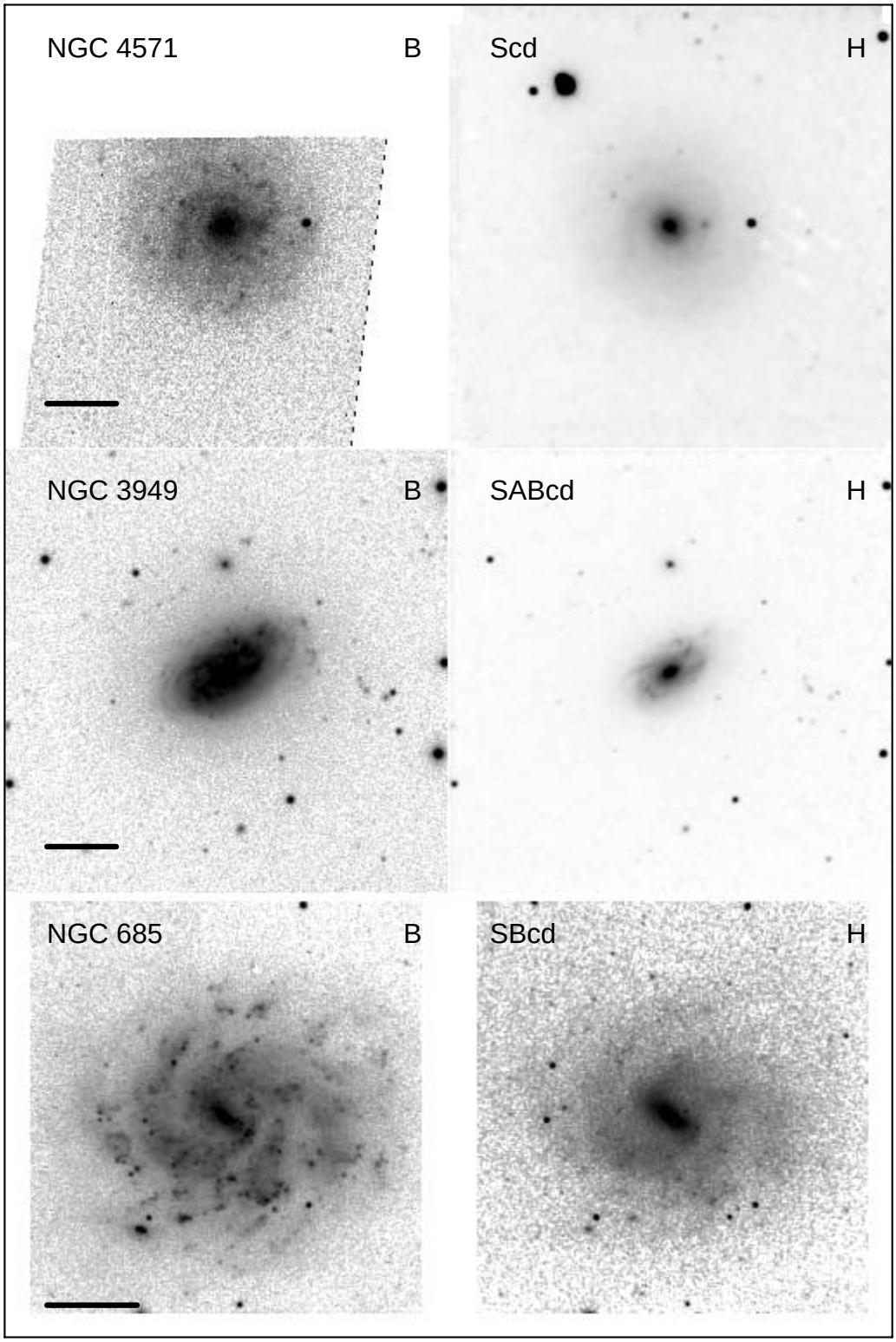


FIG. 3*h*

NGC 1309.—SABb: Small, bright, circular bulge; bulge becomes more elliptical at larger radii. No other indication of a bar. Flocculent, multiarmed spiral pattern. Spiral arms very patchy and knotty. Arms stronger to the NE than the SW. Most prominent arm appears to continue south on the SE side of the galaxy, tracing out a series of bright knots in a straight, due south line. The optical types for this galaxy are SA(s)bc: (RC3), Sc(s)II (CAG), and Scd (OSU *B*). The substantially earlier type in the near-IR is due to the enhanced prominence of the bulge in the *H* band compared to the optical.

NGC 1317.—SB0 (type example—see Fig. 3*a*): Nuclear point source embedded in a nuclear bar. Inner isophotes of the bulge are elliptical with the same major axis as the bar,

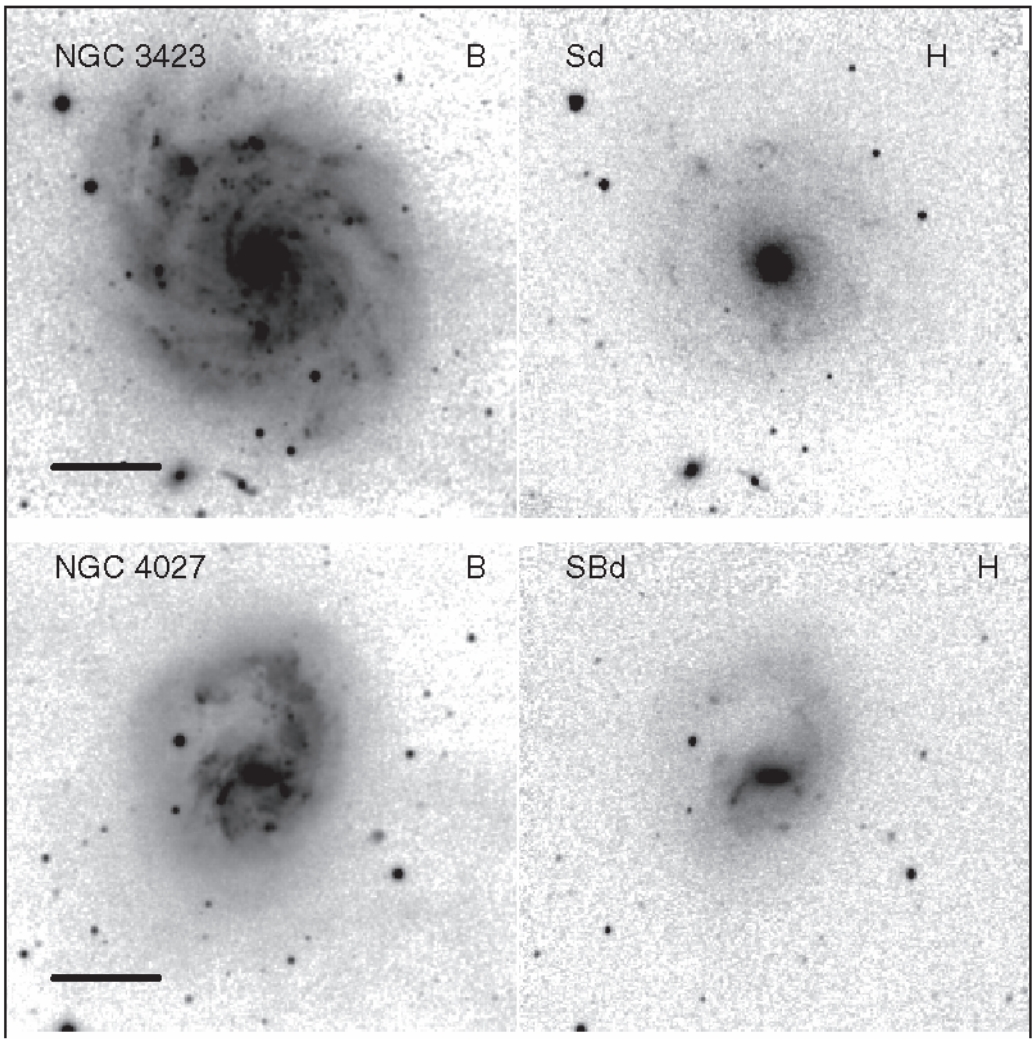


FIG. 3*i*

but much less flat. At lower intensity the bulge becomes circular. At lower intensity still, the isophotes become elliptical again, but the major axis is roughly perpendicular to the major axis of the nuclear region. This appears to extend into a second, very faint, large-scale bar (again roughly perpendicular to the inner bar). The disk is of quite low surface brightness and has a faint inner ring at the radius where the outer bar fades away.

NGC 1350.—(R)SB(r)a (type example—see Fig. 3*c*): Bright nuclear point source. Elliptical bulge, oriented with the major axis nearly N-S. Bar, with major axis skewed NE-SW from bulge major axis. Bar most obvious from bright ansae at bar ends. These bridge into an inner ring (or tightly wound spiral arms). Faint, LSB spiral features emerge from the ring at the ends of the apparent major axis and wrap to form an outer ring.

NGC 1371.—SAB(r)a (type example—see Fig. 3*c*): Bright, centrally condensed bulge. Elliptical, and oriented NW-SE at high light levels. At lower light levels, a bar is apparent, and the isophotes twist clockwise. Low surface brightness arms emerge from ansae at the bar ends. Pitch angle fairly steep. No obvious knots in arms. Arms appear to wrap around to form a faint outer ring.

NGC 1385.—SBdm (type example—see Fig. 3*j*): Faint, small bulge, with stubby nuclear bar threading it. Patchy, flocculent spiral arms emerge from several locations in the inner disk. The inner arms, especially are full of star-forming knots. Inner arms include two straight segments heading just east of north from the bar area. Outer disk is asymmetric, with very little emission on the NW side of the galaxy.

NGC 1421.—Sc: System close to edge-on. Bright symmetric nucleus embedded in an elliptical bulge. There appears to be a diffuse bar with a P.A. offset $\sim 30^\circ$ from the bulge P.A. Two spiral arms emerge from the bar feature. The arms are very well defined, but the pattern is quite asymmetric. The disk P.A. is $\sim 0^\circ$. The south arm emerges from the bar, then bends slightly to the south, and goes south in a straight line almost all the way to the edge of the disk. It is thin, HSB, and well defined. It has several strong knots/clumps of star formation along it. The arm bends to the east at the southern edge of the disk and quickly fades. The south side of the disk (east of the arm) is knotty and shows signs for one or two lower surface brightness armlets. The northern arm bends smoothly to the west from the bar, then bifurcates. The inner (western) segment is thick and has a number of bright knots, before terminating abruptly at a very elon-

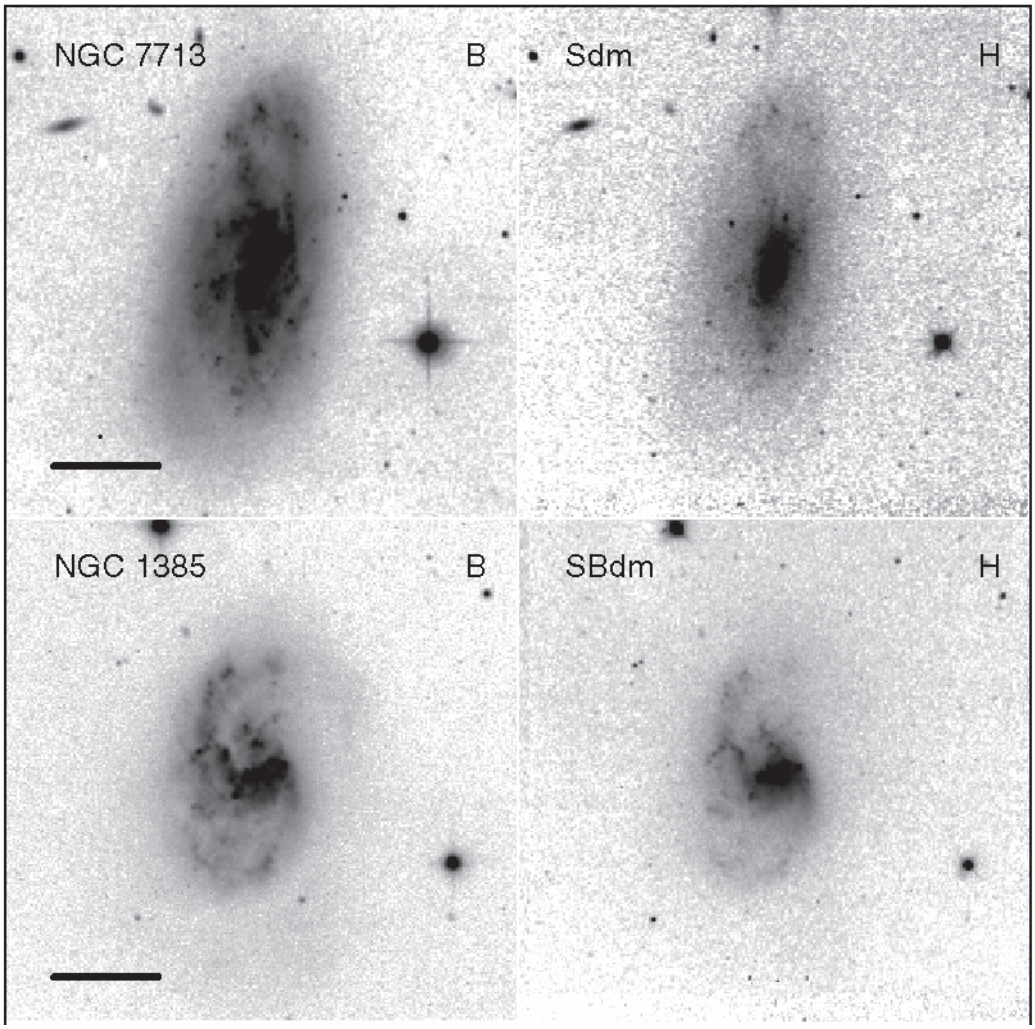


FIG. 3*j*

gated bright feature. The outer segment is smooth and of LSB. It extends approximately as far to the north as the southern arm does south but is much less well defined.

NGC 1425.—No data.

NGC 1433.—No *JHK* data.

NGC 1493.—SBb: Nuclear point source embedded in elliptical bulge with a small, high-contrast bar. Flocculent spiral pattern emerges, with structure apparent starting at the ends of the bar. The arms are moderately tightly wound. Arms have many bright knots, and at low light levels there is evidence for up to four arms, each with multiple segments.

NGC 1511.—SBd?: Nearly edge-on. SW side of bulge is hidden by a prominent dust band, indicating that the bulge is small. Inner SE spiral arm has several very bright star-forming knots. Arms do not appear very extended (may be due to foreshortening), but there is an extended, featureless LSB disk beyond the arms.

NGC 1559.—SBcd (see Fig. 4*e*): Moderately inclined. Elliptical nucleus extends into short, high surface brightness bar. Bar is thicker in the middle than at the ends. This is the only sign of a bulge. Flocculent spiral pattern, with evidence for at least three patchy arms. Arms are rich in star-forming knots. At low surface brightness levels there are a number of wispy extensions of the arms. In Figure 4*e*, note the patches of strong dust absorption that appear as red (*H*-band emission only) interspersed with the bright blue knots. The disk is much smoother in the *H* band than the optical.

NGC 1617.—(R)SAB0/a (type example—see Fig. 3*b*): Bright nuclear point source. Extends into slightly elliptical bulge. Weak bar. Stubby spiral features emerge from the bulge but quickly fade into the overall disk emission. Disk is slightly asymmetric: The major axis P.A. is roughly 100° east of north; the disk is slightly less extended to the north than to the south. Disk is very smooth, with no evidence of star-forming knots. Disk terminates abruptly at an outer ring.

NGC 1637.—SBb (pec): Fairly weak bar, extending from the major axis of an elliptical bulge. Bar is oriented close to E-W. Disk is highly asymmetric; much more extended to the NE than the SW. West arm turns to the south and wraps 270° before fading away. East arm turns to the north, and fads after only 180°. Arms fairly well-defined, with a much higher surface brightness on the east side.

NGC 1703.—SABb: System close to face-on. Symmetric nuclear source embedded in a circular bulge. Two-armed grand-design spiral pattern with arms emerging from the bulge. Arms are smooth and well-defined for ~180°, then

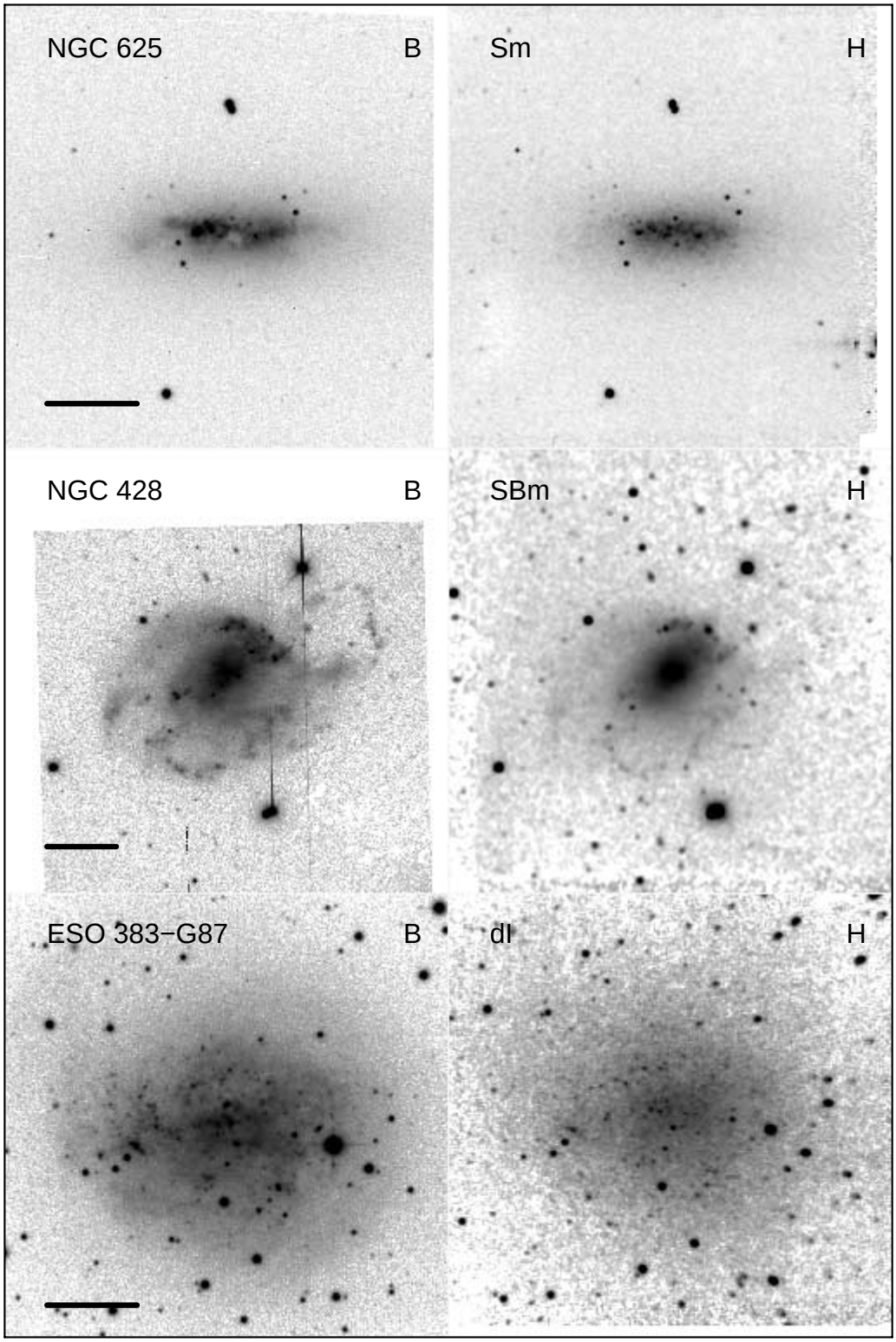


FIG. 3*k*

become diffuse and patchy. One arm can be traced through a full 360°. The other fades out after ~270°.

NGC 1792.—Sbc: Centrally condensed, elliptical bulge, with no evidence for a bar. Flocculent spiral pattern with at least five visible arms. Arms are very prominent, and full of star-forming knots. There is an asymmetric feature to the SE at low surface brightness: One of the arms does not curve in the same sense as the others, but instead extends practically straight along the major axis of the disk.

NGC 1808.—SBa: Very bright nuclear point source embedded in a short, faint bar that is further embedded in a boxy bulge, with a short, faint bar. At high surface brightness, bulge has a "lemon" morphology. At lower surface brightness, the bulge becomes strongly boxy. Spiral arms



FIG. 4*a*

FIG. 4.—Color-composite images of representative galaxies. Blue shows the *B* band, green the *R* band, and red the *H* band. (*a*) NGC 4314, (*b*) NGC 7217, (*c*) NGC 4254, (*d*) NGC 4579, (*e*) NGC 1559, (*f*) NGC 7418.

emerge from the east and west corners of the bulge. The east arm has a few bright knots near the bulge, and a diffuse patch of high surface brightness farther out. The west arm forms a very sharp, well-defined ridge and does not appear to have any knots. The arms are both embedded in a smooth disk.

NGC 1832.—SBab: Bright nuclear point source, embedded in an elliptical bulge/stubby bar. Bright ansae at the ends of the bar. Bulge is embedded in a lens. Two loosely wrapped arms emerge from the ends of the bar. West arm is very diffuse, and broad. East arm is better defined. Both arms fade from view after winding less than 180°. Arms are patchy but show no signs of star-forming knots. The optical types for this galaxy are SB(r)bc (RC3), SBb(r)I (CAG), and SAB(r)c (OSU *B*). The substantially earlier type in the near-IR is due to the enhanced prominence of the bulge in the *H* band compared to the optical.

NGC 1964.—(R)Sab: Foreground star ~4″ from galaxy nucleus. System is fairly inclined. Bright nuclear point source embedded in a thin, HSB bar within a bright elliptical bulge. At lower surface brightness, the bar and foreground star make the bulge isophotes appear lemon-shaped. Faint, smooth spiral arms emerge from the minor-axis ends of the bulge and wrap for only ~90° before fading into a general inner disk. The inner disk has a number of knots and patches. There is a faint outer disk, with a patchy outer ring structure.



FIG. 4*b*

NGC 2090.—Sb (type example—see Fig. 3*e*): Centrally condensed bulge, with no evidence of a bar. Two-armed, grand-design spiral. Arms are well defined and wrap more than 360° before fading. Outer arms become patchy. Only a few knots in the inner arms.

NGC 2139.—SBdm: No bulge. Asymmetric bar, oriented E-W (west end is brighter than east end). Diffuse, patchy LSB spiral features appear very disorganized. Direction of arm winding appears to change from the inner to the outer disk. Two-armed pattern appears in outer disk. Disk (and outer arms) has numerous star-forming knots.

NGC 2196.—S0/a: Bright nuclear point source embedded in bright elliptical bulge. A very low surface brightness disk surrounds bulge. The disk is smooth, with only a hint of some patchiness in the NW.

NGC 2207.—SB0/a: Interacting pair with IC 2163. NGC 2207 is the western system. Very bright, elliptical bulge, with short, high surface brightness arms appearing roughly perpendicular to the inner major axis. Very extensive low surface brightness arm/ring features probably caused by tidal interaction with companion to the east. LSB arms have many star-forming knots. In the SBc interpretation, the stubby arms form ansae at the end of an LSB bar.

NGC 2280.—SBbc: Small bright nucleus embedded in a short, faint bar. Spiral arms emerge from the minor axis ends of the bulge. Within the inner disk the arms are HSB and narrow. They abruptly become LSB and diffuse at the edge of the inner disk. Both arms are smooth. The east arm can be traced through ~540°. The west arm fades after ~360°. The outer arms are knottier than the inner arms.

NGC 2442.—SBbc: Bright nuclear point source embedded in a small, very elliptical bulge. Outer bulge isophotes become boxy (actually rhomboid). Spiral arms emerge from the obtuse corners of the rhombus. Spiral arms are rich in star-forming knots. Dust lanes still visible in the *H* band. The arms are asymmetric. The north arm emerges

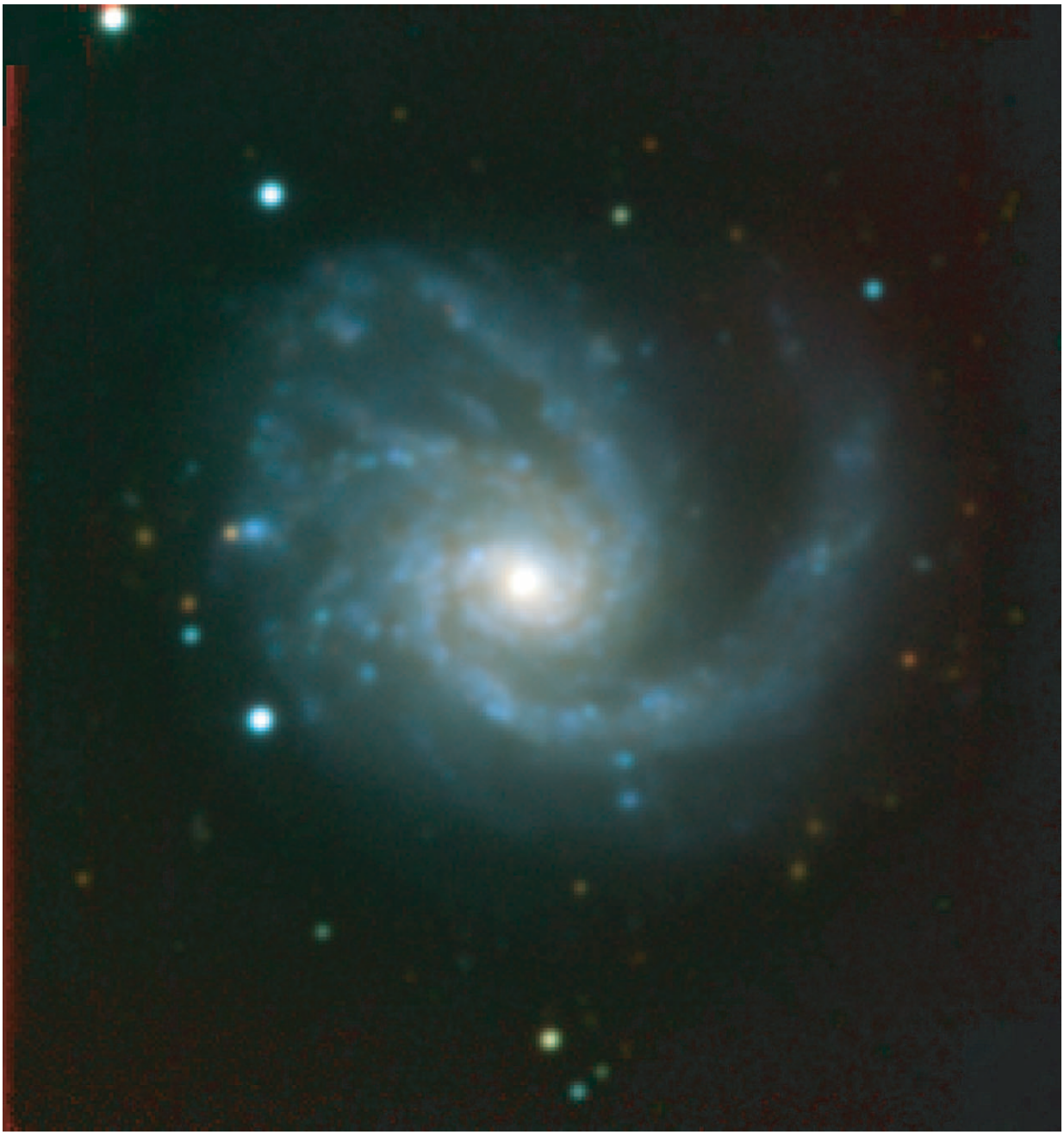


FIG. 4*c*

from the east corner of the bulge, is nearly straight for some distance, and then bifurcates, and turns sharply to the west (the bending angle is $\sim 120^\circ$). The south arm is straight, with a narrow central ridge line for even farther, and then bends sharply to the east (the bending angle is $\sim 150^\circ$), and becomes quite diffuse and broad. It appears to bend entirely back on itself at low intensity level.

NGC 2559.—SBb: Small elliptical bulge, with variable position angle: central isophotes are oriented roughly N-S. At lower intensities, the P.A. rotates to NE-SW. Prominent bar at same orientation as outer bulge isophotes. Two-armed spiral pattern, with the arm emerging from the ends of the bar. Both arms are peculiar, with abrupt kinks in several places. East arm has a handful of bright star-forming knots. West arm appears smooth. The optical types for this galaxy are SB(s)bc: pec (RC3) and SABcd? (OSU *B*). The substantially earlier type in the near-IR is due to the heavy dust obscuration in the central part of the galaxy, which conceals much of the bulge visible in the *H* band.

NGC 2566.—(R)SBa: Nuclear point source embedded in a large slightly elliptical bulge. Bulge is threaded by a long, thin, bright bar. Underlying LSB disk, with an outer ring/tightly wound spiral arms. The ring is irregular and lumpy but has no obvious bright knots of current star formation. The disk P.A. is offset $\sim 30^\circ$ away from that defined by the bar. The outer disk isophotes appear offset from the nucleus of the galaxy. However, sky irregularities make the disk hard to characterize.

NGC 2775.—S0/a: Very bright nuclear point source embedded in large slightly elliptical bulge. Disk extends

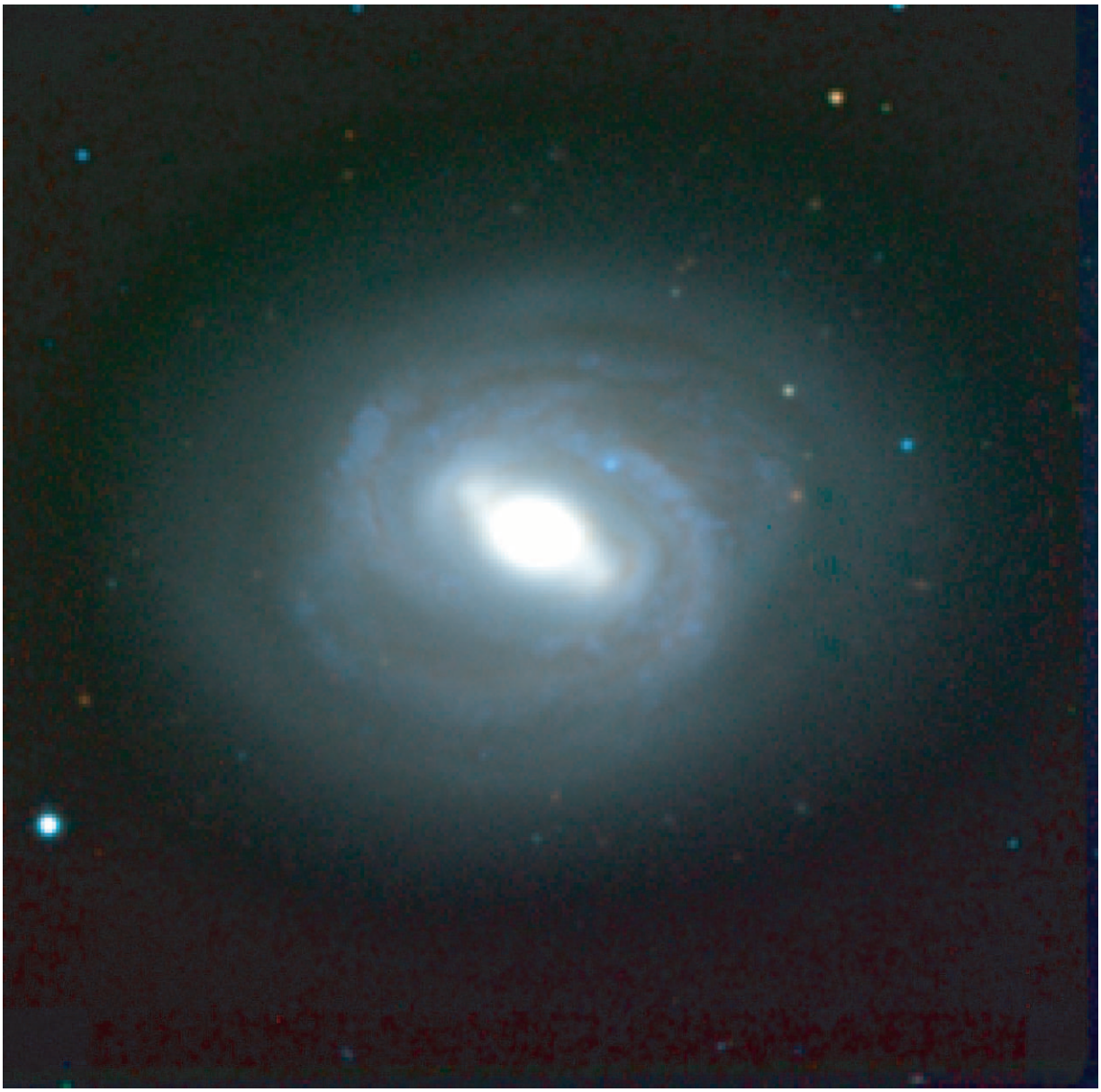


FIG. 4*d*

from bulge with nearly the same isophotal shape. There is evidence for two very faint, symmetric spiral dust absorption bands in the outer disk.

A0908-08.—Sc?: System nearly edge-on. Bright, very flattened nucleus, but no sign of a bar. The inner disk is patchy, with a number of bright knots. It is clearly crossed by a dust lane on the east side. There is a clear break between the inner and outer disks, and the major axis P.A. of the disk changes at this surface brightness discontinuity. The high inclination makes any spiral pattern hard to detect.

NGC 2964.—SABb (pec): Slightly elliptical bulge, with possible evidence of a weak bar oriented close to bulge minor axis. Four-armed spiral pattern, with two arms emerging from ansae at the bar ends, and two others emerging near the center of the bar. Arms are irregular, with the outer disk having roughly rectangular isophotes. The two arms coming off the bar ends (the north and south arms) are of higher surface brightness than the other two. There is some evidence for bright knots in all but the west arm.

NGC 3059.—SBcd: Small, very flattened bulge, threaded by a short, thin, HSB bar. Two loosely wrapped, smooth, LSB arms emerge from the ends of the bar. NW arms is much less curved than SE arm. Outer disk isophotes are roughly circular.

NGC 3166.—SB0: Very bright, very elliptical nuclear region, extending into similarly flattened bulge with the major axis oriented nearly E-W. LSB bar oriented along bulge minor axis. At fainter isophotes, the bulge engulfs this bar and becomes nearly circular. At still fainter isophotes, the bulge recovers its original E-W major axis and becomes quite boxy. Beyond this, there is an LSB disk, with no evidence for spiral features or star-forming knots.

NGC 3169.—S0/a: Very bright, flattened nucleus, with evidence for a weak bar, embedded in a luminous elliptical bulge. Outer bulge isophotes appear slightly boxy. There is a LSB disk with patchy, flocculent spiral features. No clear arm pattern. Although the disk is not HSB, it is large—perhaps overfilling the field of view. The optical types for

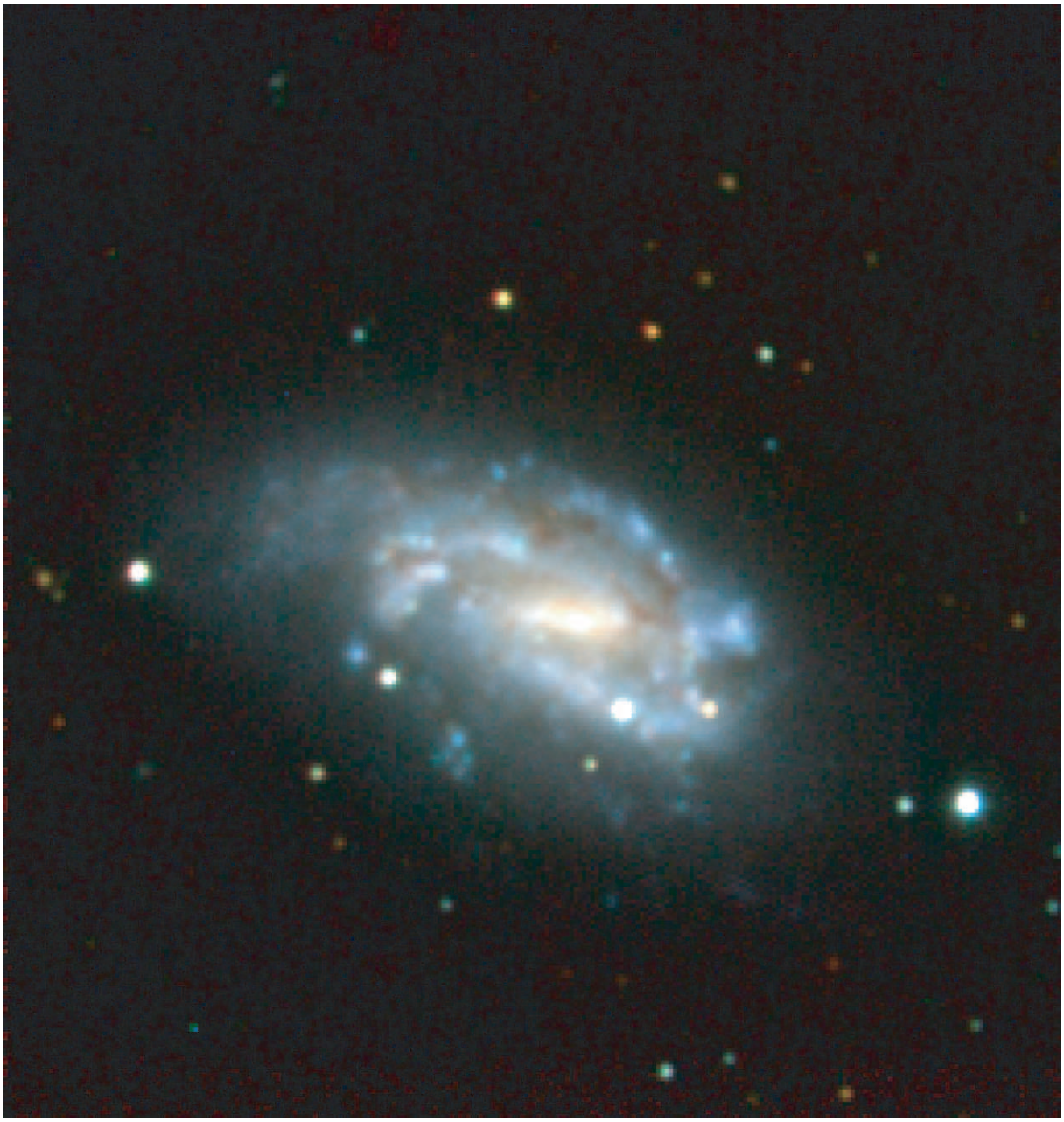


FIG. 4*e*

this galaxy are SA(s)a pec (RC3), Sb(r)I–II tides (CAG), and Sb (OSU *B*). The substantially earlier type in the near-IR is due to the enhanced prominence of the bulge in the *H* band compared to the optical and the lack of any visible spiral structure in the *H* band.

NGC 3223.—Sa: Bright nuclear point source, embedded in large, elliptical bulge. Faint, symmetric, tightly wrapped two-armed spiral pattern emerges from bulge. Arms have a few bright knots in them.

NGC 3227.—SBab: Interacting pair with NGC 3226, with overlapping disk isophotes. NGC 3227 is the system to the SE. Bright nuclear point source, embedded in a bulge with a clear X-distortion (Whitmore & Bell 1988) in the inner isophotes. The outer bulge isophotes are peanut-shaped. A bar threads the bulge, along its major axis. The P.A. of the bulge and bar is in the direction of the SE system. There are a number of star-forming knots on the SE side of the bar. Two broad, smooth, diffuse spiral arms emerge from the ends of the bar and can be traced for $\sim 180^\circ$.

NGC 3261.—SB(r)a: Bright, centrally condensed nucleus, threaded by a low surface brightness bar. Ends of the bar intersect two (even lower surface brightness) arms. The arms do not commence at the ends of the bar, but instead form a nearly complete inner pseudoring. Beyond the bar, the arms break away from the ring and can be traced for more than 180°. They are diffuse and have obvious kinks in several places. The east arm has a well-defined ridge line for $\sim 120^\circ$ past the end of the bar, and then turns sharply and becomes very diffuse. The west arm is never so well defined, but can be traced significantly farther before it fades away.

NGC 3275.—SB(r)ab: Very bright nucleus embedded in an elliptical bulge with a short bar. The bulge is embedded in a lens that extends to the ends of the bar. Faint spiral arms emerge from bar ends. Arms have no evidence for



FIG. 4*f*

knots. At high surface brightness, the major disk of the galaxy is aligned with the bar (P.A. is $\sim 135^\circ$), but at lower surface brightness, the P.A. is closer to 0°.

NGC 3319.—SBd: No bulge. Nuclear point source embedded in thin HSB bar. The point source is SW of the bar center. There are a number of other lumps along the bar. Two-armed, grand-design spiral pattern emanates from the ends of the bar, but arms are LSB. Arms can be traced through $\sim 240^\circ$ before fading. The knots are mainly in the outer parts of the arms: The inner disk is quite smooth. The south arm has many more bright knots than does the north arm.

NGC 3338.—SAB(r)b: Nuclear point source embedded in small elliptical bulge. There is a clear inner ring, with the spiral arms coming off the ring. There is a two-armed spiral pattern, but both arms appear to originate from the same spot on the ring. The arms have different inner pitch angles and appear symmetric at large radius. Although there are a few knots in disk, they are not associated with the spiral arms. The arms are smooth. They are narrow and well defined at small radii, and become broad and diffuse after winding for $\sim 180^\circ$. At faint levels, the arms can be traced for another $\sim 180^\circ$ before fading into the sky.

NGC 3423.—Sd (type example—see Fig. 3*i*): Very close to face-on. LSB, slightly elliptical bulge embedded in very LSB disk. There are traces of spiral structure in the disk, but no large-scale arms. There are also numerous star-forming knots distributed about the disk that do not lie on any of the spiral segments.

NGC 3504.—(R)SB(r)a: Bright nuclear point source in a small slightly elliptical bulge. Bulge is threaded by a thin, well-defined bar. Ansae at the ends of the bar form the base of the spiral arms. The arms wrap into an inner ring and then peel off to form a broken outer pseudoring. There are a few knots in the ansae, but little other evidence of ongoing star formation.

NGC 3507.—SBb: Nuclear point source embedded in elliptical bulge. The bulge is threaded by a prominent bar. Grand-design two-armed spiral pattern, with the arms emerging at right angles to the ends of the bar. The arms are well defined, and generally smooth, although there are some knots in the inner arms. The arm emerging from the SE end

of the bar is more tightly wrapped than that emerging from the NW end. The surface brightness of both arms drops abruptly after $\sim 180^\circ$. The arms can be traced through another $\sim 180^\circ$ before they fade into the sky.

NGC 3511.—SABbc: Fairly weak bulge with evidence for a double nucleus. Bulge is elliptical, but the galaxy is at high inclination, so this may be a projection effect. Two-armed grand-design spiral pattern emerges from the bulge. Arms are very diffuse, thick, and patchy. There are knots, but none are very prominent. At low surface brightness there are short bits of other arms.

NGC 3513.—SBc: Flattened nuclear source embedded in a thin, HSB bar. Broad ansae at the ends of the bar have a P.A. slightly skewed from that of the bar. The spiral arms emerge from the ansae. The arms are broad, and patchy, but well defined. They contain several obvious knots of star formation. The arms can be followed through $\sim 180^\circ$. They are not quite symmetric, with the south arm being more open than the north arm, and the north arm showing signs of more vigorous star formation.

NGC 3583.—SBc: Bright nuclear source, embedded in an elliptical bulge. Bulge is threaded by a prominent bar with a P.A. roughly halfway between that of the bulge major and minor axes. Spiral structure commences at the radius of the bar ends but is quite peculiar. One arm appears to originate near the NW major-axis end of the bulge. It is quite diffuse here. As this arm crosses the P.A. of the bar, it becomes better defined and brighter. It then continues to the SE, but rapidly becomes diffuse, and fades away. A second arm appears to commence from the SW end of the bar and wraps very tightly around the south side of the bulge. A very low surface brightness spur of this arm extends to the east, making the system a three-armed spiral. When the second arm crosses the P.A. of the bar on the east side, another arm commences, and runs parallel to the second arm to the NW (that is, the second arm has a double structure once it passes the SW end of the bar). At low surface brightness, the arms become very diffuse.

NGC 3593.—S0/a: System close to edge-on. Bright central point source embedded in a flattened luminous bulge. Disk extends from the bulge with same P.A. There is patchy extinction in the inner disk. No evidence of any spiral pattern in the disk.

NGC 3596.—SABb: Nuclear point source embedded in a slightly elliptical bulge. Oval inner disk aligned with bulge P.A. Two-armed spiral pattern emerges from the major-axis ends of the bulge. North inner arm is higher surface brightness than south arm. Arms have ridges of higher surface brightness with lower surface brightness extensions outward. Both arms can be traced for 270°–300°. Arm pattern on south side of the disk is complicated, with breaks appearing in the ridge line of the arm.

NGC 3646.—SABab pec: Nuclear point source embedded in a small, very flattened bulge. An asymmetric inner disk surrounds the bulge. The inner disk is more extended to the NW than to the SE. The NW side of the inner disk has a number of knots. The spiral pattern is very odd. One spiral arm emerges from the SE end of the inner disk and turns counterclockwise. Another emerges from the NW side of the inner disk and turns clockwise. These two arms appear to merge on the SW side of the galaxy, joining in a point. The arm structure on the west side is very well defined, and HSB, with many bright knots. On the east side, the arms are diffuse and patchy, with fewer knots. There is an LSB outer disk on the west side. The referee suggests, and we agree, that this may be an example of a galaxy with visible leading and trailing arms.

NGC 3675.—SB(r)a: Bright nuclear point source embedded in an elliptical bulge, threaded by a low-contrast bar. Narrow, tightly wound spiral arms form an inner pseudoring and can be traced for another full winding outside the ring. Arms are embedded in a clear interarm disk. The outer arms are very patchy and filamentary.

NGC 3681.—SB(r)0/a: Nuclear point source, threaded by short nuclear bar. The bar causes the bulge isophotes to be very elliptical. Bulge is embedded in a smooth inner disk, with a complete inner ring at its edge. The disk surface brightness drops abruptly outside of the ring. The outer disk is LSB, and smooth, with no evidence of any spiral structure. The optical types for this galaxy are SAB(r)bc (RC3), SBb(r)I–II (CAG), and SAB(r)b (OSU *B*). The substantially earlier type in the near-IR is due to the lack of obvious spiral structure in the *H* band.

NGC 3684.—SABb: Small, elliptical bulge, threaded by a prominent bar. Two-armed grand-design spiral pattern with arms emerging from the major-axis ends of the bar. Arms are fairly low contrast. There are some knots, especially on the west arm, but the arms are fairly smooth. Both arms can be traced through $\sim 300^\circ$ before the fade into the sky.

NGC 3686.—SBbc: Bright nuclear point source embedded in a very elliptical bulge. Bulge is threaded by a weak bar, with the bar P.A. skewed $\sim 30^\circ$ from the bulge major axis. Grand-design two-armed spiral pattern emerges from the ends of the bar. Inner arms are high-contrast and have lots of filamentary structure. After winding $\sim 140^\circ$, the arms become diffuse and LSB. The arms can be traced through almost a full 360°. South arm bifurcates near the bar end, with the outer part being LSB and diffuse. Thus, the system is three-armed at large radii and LSB levels.

NGC 3705.—SAB(r)ab (type example—see Fig. 3*d*): Star only $\sim 3''$ from nucleus. Nuclear point source embedded in an elliptical bulge. Low-contrast bar threads bulge along the bulge minor axis. Bar ends on a high-contrast asymmetric inner ring. Weak spiral pattern in the disk outside the ring. The arms are patchy and narrow.

NGC 3726.—SB(r)bc: Nuclear point source embedded in small very elliptical bulge. Bulge is threaded by long, prominent bar. The bar ends at an inner ring. The P.A. of the ring is skewed by $\sim 30^\circ$ from the bar major axis. Three spiral arms emanate from the ring, with the north arm being the best defined. It can be traced for $\sim 150^\circ$. The south arm is the brightest and contains the majority of the star-forming knots. It is very broad at its base and not well defined. It fades after only $\sim 90^\circ$, but an LSB extension can be traced for another $\sim 90^\circ$. The third (east) arm is very patchy and diffuse. After emerging from the east side of the ring, its inner portion proceeds in a nearly straight line to the NNW and then bends sharply after $\sim 90^\circ$. The bend is a $\sim 140^\circ$ turn to the SW. There are several bright knots on this part of the arm. The rest of the arm forms a very broad LSB feature to the north and NE of the galaxy. Because of this, the system is very asymmetric at low surface brightness levels.

NGC 3810.—SABbc: Nuclear point source embedded in large, slightly elliptical bulge. Two-armed spiral pattern emerges from the bulge, with well defined, high-contrast inner arms. The arms become patchy, diffuse, and irregular after winding $\sim 90^\circ$. They split into at least four outer arms. Even the outer arms are rich in bright knots.

NGC 3877.—Sbc?: System close to edge-on. Bright elliptical nuclear source embedded in a small, less elliptical bulge. Inclination and obvious dust extinction make the details hard to see, but there is an open two-armed spiral pattern. The disk is full of bright knots.

NGC 3885.—S0/a: Bright, very elliptical bulge, with a possible nuclear bar. Bulge becomes boxy at lower surface brightness. Stumpy spiral features protrude from the NW and SE corners of the bulge but disappear very rapidly. A low surface brightness disk extends from the bulge and shows weak patchy features that may be bits of arm structures. No evidence for star formation.

NGC 3887.—SBab: Fairly small, centrally condensed bulge, becoming very elliptical with increasing radius. Bulge is threaded by a bar with nearly the same P.A. as the bulge major axis. Two-armed spiral pattern commences at the bar ends. The arms can be traced for $\sim 300^\circ$ before disappearing. The arms do not have knots, but they are quite lumpy (features much larger than typical star-forming knots). Beyond $\sim 180^\circ$, the arms are traced mainly by these lumps (the diffuse emission is largely lost in the sky).

NGC 3893.—SABbc: Centrally condensed, slightly elliptical bulge. Grand-design two-armed spiral pattern emerges from the major-axis ends of the bulge. The inner arms are high-contrast, rich with star-forming knots, and have obvious inner dust lanes. After winding for $\sim 250^\circ$, they become broad, LSB outer arms that can be traced for another $\sim 100^\circ$ before fading into the sky.

NGC 3938.—Sb: System nearly face-on. Centrally condensed nucleus in a bright bulge. Grand-design two-armed spiral in the inner disk, with the arms bifurcating and becoming very broad in the outer disk. Arms are very knotty. They can be traced through at least a full 360° before fading into the sky.

NGC 3949.—SABcd (type example—see Fig. 3*h*): Very elliptical bulge. Irregular, flocculent spiral structure in disk, with many filaments, and knots of star formation.

NGC 4027.—SBd (type example—see Fig. 3*i*): No bulge. Nucleus embedded in a bar. Two spiral arms emerge from the end of the bar. South arm is short, winds less than 90° before fading, and has several large, bright knots of star formation. North arm is diffuse and broad, but winds through nearly 180° before fading. No obvious knots in outer north arm. South arm, and the beginning of north arm, are embedded in a diffuse, patchy disk.

NGC 4030.—Sab: Centrally condensed nucleus embedded in a large elliptical bulge. Flocculent spiral pattern, with at least three arms. Arms are patchy and wispy, still showing signs of dust lanes in the *H* band. Inner disk has many star-forming knots. Outer disk appears quiescent.

NGC 4038.—S pec: North system of the Antennae. Knotty nuclear region, with one prominent arm emerging on the SW. Arm curves around to the north and breaks up into a rich array of star-forming knots on the SE side, as the arm approaches the southern system.

NGC 4039.—S pec: South system of the Antennae. Nuclear point source. Weak arm emerges on the SW and quickly fades into an LSB smear. NE side becomes rapidly confused with the star-forming bridge from the north system.

NGC 4051.—SBb: Bright nuclear point source embedded in an elliptical bulge. Bulge is threaded by a prominent bar aligned with the bulge major axis. System has a complex, multiarm spiral pattern, with two dominant arms that emerge from the ends of the bar. There are also two fainter arms. One emerges from the west end of the bulge. The other appears to form via the bifurcation of the southern main arm. The arms are rich in substructure and star-forming knots.

NGC 4062.—Sb: Small, moderately elliptical bulge. High-contrast, grand-design spiral pattern, with the arms emanating from the minor-axis ends of the bulge. Arms are narrow and smooth for the first 180°, then become diffuse and filamentary. Both arms can be traced through a full 360 winding.

NGC 4100.—SBbc: System close to edge-on. Bright nucleus offset to the west of the center of the outer bulge isophotes. Bulge is threaded by a narrow, well-defined bar. Initially two-armed spiral pattern begins from bar ends. Arms bifurcate after winding for $\sim 180^\circ$. Arms are fairly smooth, with a few knots on the south side. Arms embedded in a smooth, LSB disk.

NGC 4123.—SBb: Nuclear point source embedded in a very elliptical bulge. Bulge has a prominent X-distortion, and boxy/peanut-shaped outer isophotes. A long, high-contrast bar threads the diagonal of the boxy bulge. Bar is asymmetric, with the east side being narrower, and higher surface brightness. Two-armed spiral pattern emerges from the ends of the bar. The arms are very wispy and patchy. They can be traced for $\sim 180^\circ$ before fading into the sky.

NGC 4136.—SB(r)a: Small, centrally condensed bulge, threaded by a short, thick bar. Bar ends on a full, high-contrast inner ring. The major axis of the ring is nearly orthogonal to that of the bar. Two open, LSB spiral arms emerge from the major axis ends of the ring and can be traced through $\sim 120^\circ$ before fading. The south arm is fainter than the north arm. Most of the bright knots are associated with the interarm disk. The optical types for this galaxy are SAB(r)c (RC3), Sc(r)I–II (CAG), and SAB(r)bc (OSU *B*). We classify NGC 4136 substantially earlier in the *H* band because the outer, open spiral arms are very faint in the near-IR, leaving the inner arm/ring structure as the spiral feature that dominates the classification.

NGC 4145.—SBc (type example—see Fig. 3*g*): Foreground star or offset nuclear point source on SE end of a diffuse nuclear bar. If it is a foreground star, there is no nucleus. Bar is embedded in a large elliptical bulge with an outer P.A. skewed $\sim 45^\circ$ from that of the bar. Spiral arms emerge from the ends of the bulge, at a very acute angle. Arms are very diffuse and filamentary but can be traced for $\sim 270^\circ$ before fading into the sky. Many star-forming knots in the outer disk.

NGC 4151.—SB0/a: Very bright nuclear point source (AGN) embedded in a large, bright, circular bulge. Bulge is threaded by a large, thick, high-contrast bar. Weak ansae at the bar ends. No evidence for spiral structure. No evidence for star formation.

NGC 4178.—SBc?: System nearly edge-on. No nucleus or bulge, but a long, high-contrast bar. Two broad, low-contrast spiral arms emerge from the ends of the bar. These fade into the ambient disk after $\sim 120^\circ$. There are three very bright star-forming knots on the SW side of the galaxy, with many fainter ones throughout the disk.

NGC 4212.—SABbc: Nuclear point source embedded in an elliptical bulge. There is a smooth inner disk from which two spiral arms emanate. The west arm has higher contrast and more knots. It can be traced for $\sim 180^\circ$ before fading. The east arm is much lower surface brightness but can be

traced ~270° before fading. As the east arm turns to the north, this gives the outer disk a strong north asymmetry. Dust lanes are clearly visible in the east arm.

NGC 4242.—SBm: Faint nuclear point source embedded in a very low surface brightness disk. The central disk is elongated and at considerably higher surface brightness than the outer disk. The outer disk is very LSB. It has a few patches and knots, but no sign of spiral structure.

NGC 4254.—SABc (see Fig. 4*c*): Small circular bulge. Disk has an asymmetric spiral pattern. The spiral arm pattern is complex. There are three prominent arms, and a weak fourth arm. Two of the arms begin at the SW end of the bulge. One of these wraps tightly around the bulge, and the other is more open. The third bright arm begins at the NE end of the bulge. The inner SW arm is just outside the NE arm at this point. The inner SW arm then opens, and the NE arm winds inside it. There is evidence for a weak arm on the west side of the galaxy. The arms are narrow, well defined, and full of star-forming knots. At low surface brightness levels, the arm asymmetry makes the disk look very lopsided. This is a galaxy with essentially the same morphology in the *B* and *H* bands. Note in Figure 4*c* that there are no small-scale differences in the optical and near-IR.

NGC 4293.—SBab: System close to edge-on. Nuclear point source embedded in a boxy bulge with an outer X-distortion. A weak, short, broad bar threads the bulge along a diagonal. Two very open, stubby, broad spiral arms emerge from the ends of the bar. They can only be followed for ~45° before terminating abruptly at a discontinuous decline in disk surface brightness. The arms are defined by a series of bright blobs. The outer LSB disk has a P.A. skewed ~45° from that of the inner disk/bulge. It has traces of spiral structure that give it an irregular isophotal shape.

NGC 4303.—SBbc: Bright, centrally condensed circular bulge. Bulge is threaded by a faint bar that makes the outer bulge isophotes appear elliptical. System has an inner pseudoring formed by the spiral arms. Arm pattern is complex and irregular. Both arms start near the bar ends, but slightly offset from them. The south arm has a great deal of structure near its base but becomes smooth and diffuse after only ~45°. At 90° it bifurcates, with one segment turning abruptly to the west and then fading rapidly. The other segment completes the inner pseudoring on the west side. The north arm bifurcates immediately. The inner segment forms the east side of the pseudoring and continues for a total of ~240° before fading. It has star-forming knots for the first 180° and then becomes smooth and diffuse. The outer segments of the north arm form a wide series of knotty filaments to the NE. All of these fade from view after ~90°.

NGC 4314.—(R)SBa (see Fig. 4*a*): Bright, centrally condensed bulge. Inner isophotes are circular but become quite elliptical at larger radii. Bulge is boxy and is threaded by a long, prominent, narrow bar. There are clear ansae at the ends of the bar. There is a faint ring intersecting the bar ends. Two broad, diffuse, LSB spiral arms also emerge from the ends of the bar. No prominent star-forming knots exist in the arms. The arms can be traced for ~120° before fading. Note in Figure 4*a* that the only color-dependent structure in NGC 4314 is the nuclear spiral starburst that shows up strongly in the optical.

NGC 4388.—SB(r)a: Elliptical nuclear region embedded in a moderately bright bulge. System is close to edge-on. Two well-defined and tightly wrapped spiral arms form a nearly complete ring. The arms have a number of concentrations in them, but these are larger and more diffuse than typical H II region knots. At fainter isophotes this bulge/ring system begins to look like a boxy bulge embedded in a disk. There is an LSB extension to the disk beyond the arms/ring.

NGC 4394.—(R)SB0/a: Bright nuclear point source embedded in a slightly elliptical bulge. The bulge is threaded by a prominent bar. Ansae at the end of the bar form the base of a tightly wrapped inner spiral arm pattern. The arms are faint and diffuse, although there are a number of star-forming knots visible. The NE arm is more prominent than the SW arm.

NGC 4414.—Sab: Bright nuclear point source embedded in a small elliptical bulge. Inner disk has a different P.A. than the bulge. Spiral features appear in the inner disk and are brightest here. The disk is very knotty, with evidence for many bits of arms. Spiral pattern is flocculent.

NGC 4448.—SB(r)a: Very elliptical bulge, threaded by a prominent bar that is nearly perpendicular to the bulge major axis. Two-armed spiral pattern, with arms beginning at the ends of the bar. Arms are very tightly wrapped, forming a compete inner pseudoring. System is close to edge-on and shows evidence for a dust lane along the north side (galaxy major axis is very close to E-W). Both arms bifurcate after only ~30°, with the inner, HSB portions forming the pseudoring. The outer arms are much lower surface brightness but can still be traced for ~180° before fading.

NGC 4450.—SBab: Nuclear point source embedded in a luminous elliptical bulge. The bulge is threaded by a wide high-contrast bar, with a P.A. ~20° offset from that of the bulge. Two tightly wrapped, narrow, low-contrast arms emerge from the ends of the bar and can be traced through several turns before fading into the ambient disk. The P.A. of the outer disk isophotes is aligned with that of the bulge and not that of the bar.

NGC 4457.—(R)SB0/a: Bright, very elliptical nuclear source embedded in a nearly circular bulge. Bulge is threaded by a weak bar. Bulge/bar system is embedded in a fairly low surface brightness disk that has a clear outer ring.

NGC 4487.—SBd: Point source nucleus offset from the center of the inner isophotes. Inner isophotes form a small bar/elliptical bulge. Disk has evidence for faint diffuse spiral features but clear arms cannot be traced.

NGC 4490.—SBm: System close to edge-on. Center of system is knotty. No nucleus, or bulge. Open, diffuse spiral arms emerge from central area but quickly fade into the ambient disk. disk is very knotty, with obvious dust lanes and patches. Outer disk isophotes are irregular, with abrupt changes in P.A. Evidence for very LSB extensions of the disk to the NW and SE.

NGC 4496A.—SBd? pec: Interacting with NGC 4496. Faint nucleus within a thin, very prominent bar. There is a hint of spiral structure to the NW (away from the brighter galaxy), but otherwise the disk is very patchy and irregular. There appear to be many luminous knots/companion galaxies. Most of these are associated with the NW system, but they exist throughout the region.

NGC 4504.—SBcd: Point source nucleus. Highly elliptical bulge, but this may be an inclination effect. Very low surface brightness arms extend from the ends of the bulge, with the P.A. being consistent with the bulge being weakly barred. No evidence of star-forming knots. Entire galaxy is very LSB.

NGC 4527.—SABab: Small, bright elliptical bulge. Outer bulge isophotes are irregular, possibly due to extinction.

Prominent grand-design two-armed spiral pattern, with the arm origin slightly offset from the bulge major axis. Arms are fairly broad, even in the inner region and show a great deal of patchy/filamentary structure. System is close to edge-on, so foreshortening is a problem, but the arms appear to continue for at least 180° before fading. The arms, and the interarm regions, are rich in star-forming knots.

NGC 4548.—SBab: Nuclear point source embedded in a slightly elliptical bulge. Bulge has a clear isophotal twist of ~90° from the inner to the outer isophotes. Bulge is threaded by a prominent bar, aligned with outer bulge P.A. There is an incomplete inner pseudoring at the ends of the bar, formed by the inner parts of the spiral arms. The arms do not begin at the bar ends, but more than 90° before that. After the arms wrap past the bar, the SE arm becomes very open and quickly becomes diffuse. The NW arm is much more tightly wrapped and remains prominent for much longer. The east arm has many more knots in its inner part than the west arm. The outer disk is asymmetric, with the SE side being higher surface brightness than the NW. The arm structure splits into several armlets in the outer disk. Outer disk isophotes are roughly aligned with the inner bulge isophotes (and orthogonal to the outer bulge).

NGC 4568.—Sbc: Interacting pair with NGC 4567. NGC 4568 is the system to the SE. Small, moderately bright elliptical bulge, embedded in an inner disk. Inner disk has structure, but no spiral arms. Arms begin somewhat farther out and are narrow, well defined, and smooth. There is a lot of interarm emission as well. There are fainter, flocculent arm structures on the north side of the galaxy.

NGC 4571.—Scd (type example—see Fig. 3*h*): Large, centrally condensed, circular bulge embedded in an inner lens. There is a faint two-armed spiral pattern emerging from the lens. The inner arms are fairly well defined. The arm beginning in the south is well defined for 150° and then becomes very faint and diffuse. The diffuse continuation can be followed for another ~150°. The north arm is well defined for ~270° but has several abrupt kinks. Beyond this, it becomes diffuse and can be traced for another ~90°.

NGC 4579.—SBa (see Fig. 4*d*): Bright, centrally condensed, slightly elliptical bulge, threaded by a prominent bar with a P.A. offset ~30° north of the bulge major axis. Bright ansae at the ends of the bar are the origins of the spiral arms. Arms are smooth, with no evidence of knots or substructure, and tightly wrapped. The arm emanating from the SW end of the bar is the more prominent and can be traced for ~300°. The NE arm can be traced for ~200°. Note in Figure 4*d* that the outer spiral structure in NGC 4579 is very blue. The difference in morphology between the optical and near-IR is driven by the very blue outer star-forming spiral arms.

NGC 4580.—S(r)b: Small circular bulge embedded in a smooth inner disk. The edge of the inner disk is defined by a prominent inner ring. The ring is formed by a pair of spiral arms that break away after turned 180°. Once past the ring, the arms break up into a flocculent spiral.

NGC 4593.—SBa: Bright nuclear point source embedded in a large elliptical/boxy bulge. A strong bar emerges from the NE and SW corners of the boxy bulge. The ends of the bar coincide with the edge of an inner disk or lens. Two very diffuse, smooth open spiral features emerge from the ends of the bar. They can both be followed for ~150°–180° before fading. There is evidence for a third arm emerging from the inner disk on the south side of the galaxy.

NGC 4618.—SBm: No bulge. Nucleus is embedded in a diffuse bar. The bar is not centered on the nucleus, but rather extends farther to the SW than the NE of the nucleus. There is one prominent spiral arm emanating from the NE end of the bar and continuing for at least 300° before fading out. The prominent star-forming knots are all in the first ~120°. Beyond this, the arm becomes smooth and very diffuse.

NGC 4643.—SB0: Bright, elliptical bulge threaded along its major axis by a long, prominent bar. Bulge/bar is embedded in a faint, smooth, featureless disk.

NGC 4647.—SBbc: Small, very flat bulge embedded in a bar with the bar P.A. nearly orthogonal to the bulge P.A. Symmetric two-armed spiral pattern emerges from the ends of the bar. Arms can be traced through a full winding before fading. Outer arms are very fluffy. May be effected by nearby giant elliptical.

NGC 4651.—SABa: Bright nuclear point source embedded in slightly elliptical bulge. Bulge is threaded by a prominent bar that is misaligned by ~30° with the bulge major axis. A complex spiral pattern begins at the radius of the bar ends, but the arms do not clearly begin at the ends of the bar. There are at least three visible, smooth, tightly wrapped, and well-defined arms. Two of them can be traced for ~150°. The third is fairly short, wrapping for only ~90°. There is a clear LSB extension of the disk, with evidence for bits of spiral structure that may or may not be associated with the more prominent inner arms. The optical types for this galaxy are SA(rs)c (RC3), Sc(r)I–II (CAG), and Sbc (OSU *B*). The substantially earlier type in the near-IR is due to the enhanced prominence of the bulge in the *H* band compared to the optical, and the very low contrast of the spiral arms in the near-IR.

NGC 4654.—SBcd: No real bulge. Nucleus is threaded by a short, thin, HSB bar. Two prominent spiral arms emanate from the ends of the bar. The arm emanating from the SE end of the bar and wrapping around the north side of the disk is the more prominent. It is rich in star-forming knots for the first ~180° and becomes smooth and diffuse thereafter. It can be traced for nearly a full 360°. The inner part of the NW arm is also rich in star-forming knots but becomes broad and diffuse after ~150°. It can be traced only ~270° before fading from view.

NGC 4665.—(R)SBa: Bright round nuclear source embedded in a luminous, slightly elliptical bulge. Bulge is threaded by a prominent, HSB bar. Two faint, diffuse spiral arms emerge from the ends of the bar and form a complete pseudoring. There is also clear interarm emission. The faint outer isophotes are clearly elliptical, at a position angle ~45° away from that of the bar.

NGC 4666.—SBc?: System close to edge-on. Bright nucleus embedded in a thin HSB bar. Bulge is small and flattened. There appears to be spiral structure emanating from the ends of the bar, but the system inclination makes the spiral pattern hard to see. Any spiral pattern is flocculent, rather than grand design. The ends of the bar and the disk are full of star-forming knots and patches of extinction.

NGC 4689.—Sb: Small, slightly elliptical bulge, embedded in a slightly elliptical, smooth inner disk. Faint spiral features emerge from this disk at the point that its surface brightness drops rapidly. The arms are very low contrast but clearly defined as ridges of changing surface brightness in a very LSB outer disk.

NGC 4691.—SBd: No real bulge. A number of bright knots are strung along a prominent bar. The brightest of these knots is somewhat elliptical, and has a different P.A. than does the bar, but is close to the bar midpoint. Two diffuse, LSB arms emerge from the ends of the bar, and form a nearly complete, faint outer ring. No evidence for knots associated with the arms.

NGC 4698.—S(r)a: System seen close to edge-on. Bright nuclear point source embedded in a large, luminous bulge. Bulge isophotes are circular. A smooth disk surrounds the bulge. There are no signs of star formation, but there are features in the disk that could be either very tightly wrapped spiral arms or a ring.

NGC 4699.—SB0: Bright nuclear point source embedded in elliptical bulge. The bulge is threaded by a short bar, oriented along the bulge major axis. The bulge/bar system is embedded in a smooth, featureless disk with the same P.A. as the bulge. No evidence of spiral structure.

NGC 4772.—(R)SB0: Nuclear point source embedded in a bright, circular bulge. Bulge is threaded by a long, broad, LSB bar. At the ends of the bar, two very faint, narrow, smooth arms wrap around the galaxy to form an outer ring.

NGC 4775.—Sd: Small, elliptical bulge. Inner disk is irregular, with no clear spiral pattern. Spiral pattern in the outer disk is very faint and asymmetric. The dominant arm is very open, broad, and diffuse. It originates on the SE side of the disk and curves to the NW. It can be traced for $\sim 180^\circ$. The arm originating on the NW side of the disk is higher surface brightness, but very short and stubby. There are obvious knots in the arms/disk.

NGC 4781.—SBdm: Small, faint bulge. A small bar is oriented nearly E-W. Very ratty, patchy, open spiral arms emerge from the ends of the bar. The disk has a P.A. skewed about 30° south of E-W (significantly different than that of the bar).

NGC 4818.—SB0/a: Bright nuclear point source embedded in an elliptical bulge. Bulge is threaded by a bar. The P.A. of the bar is skewed $\sim 30^\circ$ from the major axis of the bulge. (An alternate description is that there are short, very loosely wrapped spiral arms emanating from the bulge). At lower surface brightness, this structure simply appears to be a bulge with the P.A. of the bar. At still lower surface brightness levels, this inner structure is embedded in a faint disk. The P.A. of the disk is aligned with the P.A. of the *inner* bulge and not with the bar/outer bulge isophotes. There is evidence for very low contrast, broad spiral features in the disk.

NGC 4856.—S0/a: Centrally condensed, bright elliptical nucleus, with small variations in P.A. Bulge is very large and bright, with no sign of a bar (galaxy is highly inclined). Stubby, smooth, low-contrast arms emerge from the bulge and fade rapidly into the overall disk emission. Disk is symmetric and featureless aside from the stubby arms.

NGC 4900.—SBdm: No real bulge. Nucleus threaded by a short, HSB bar. One prominent spiral arm emerges from the SE end of the bar. Arm is very patchy and rich in star-forming knots. The arm is embedded in a patchy disk, the center of which is clearly offset from the nucleus/bar. The disk has evidence for star formation not associated with the arm.

NGC 4902.—SB(r)b: Centrally condensed bulge. Outer bulge isophotes are elliptical. A prominent bar is slightly skewed with respect to the bulge major axis. Bright stellar feature in/imposed on SW side of bar. Bar ends in a pronounced inner pseudoring. After $\sim 150^\circ$ of winding, spiral arms break away from the ring (the ring is complete, but the final $\sim 30^\circ$ on either side is much fainter). At least two fainter arms emerge earlier from the ring, the more prominent of which emerges at a clear kink on the north side of the ring. The arms are diffuse and patchy.

NGC 4930.—SB(r)ab: Bright nuclear point source embedded in an elliptical bulge, with a long, prominent bar. There is a resonance ring at the ends of the bar. Ring is slightly brighter at the ends of the bar. Faint, smooth spiral features extend from the ring but are offset in P.A. by $\sim 135^\circ$ from the bar ends (assuming trailing arms).

NGC 4939.—SABb: Nuclear point source embedded in a very elliptical bulge. Evidence for a weak bar that makes the outer bulge isophotes lemon-shaped. There is a tightly wrapped, two-armed grand-design spiral pattern, with the arms emerging from the minor axis ends of the bulge. The arms are narrow, smooth, and very well defined. They can both be traced through $\sim 540^\circ$ before fading into the sky. The arms become broader and more diffuse after the first $\sim 360^\circ$.

NGC 4941.—SABa: Marginally resolved nucleus in an elliptical bulge with a strong isophotal twist. Smooth, low-contrast, bisymmetric two-armed spiral pattern emerges from the major-axis ends of the bulge. Arms can be traced for $\sim 180^\circ$ before fading into the ambient disk.

IC 4182.—dI: Nuclear point source embedded in a diffuse, LSB disk with no sign of spiral structure, and some evidence for patchy star formation.

NGC 4995.—SBab: Elliptical bulge, threaded by a weak bar with the bar P.A. skewed $\sim 45^\circ$ from that of the bulge. Tightly wrapped spiral arms emerge from the bar ends. There are four arms, but it is really a doubled two-arm spiral, with both arms doubled from the outset. The inner arms are high contrast, with sharp ridge lines. There are a number of knots, especially on the north side of the disk. The outer disk isophotes are aligned with the bulge major axis.

NGC 5005.—SBa: System is fairly inclined. Bright, elliptical bulge with a flattened nuclear source. Bulge is threaded by a bar with a P.A. skewed $\sim 30^\circ$ from that of the bulge. The outer bulge isophotes are boxy, and the bar crosses the diagonal of the bulge. There are two ansae near the ends of the bar. Two very narrow spiral arms. The inner arms have some evidence for star-forming knots and are quite open. However, the outer arms tighten and appear to wrap several times around the system. The outer disk shows an occasional knot, but there is no coherent star-forming pattern associated with the outer arms.

NGC 5054.—SABc: Bright, round nuclear source threaded by a nuclear bar. This causes the outer bulge isophotes to appear elliptical. There is an inner disk, with no spiral structure. Beyond this, there is a prominent, grand-design three-armed spiral pattern. The arms are all well defined and have numerous star-forming knots. The arm origin points are spaced $\sim 120^\circ$ apart, so there is no evidence that this galaxy has two main arms plus an anomalous arm. The N/NE arm has the steepest pitch angle, but all are fairly loosely wound. All the arms can be followed for $\sim 180^\circ$ at the faintest level. Beyond $\sim 120^\circ$, the N/NE arm is quite faint.

NGC 5078.—Sa: System close to edge-on. Bright elliptical bulge, clearly cut by an absorption lane to the SW. (The major axis is roughly NW-SE). A feature resembling a bar is probably the edge-on disk. Very large B/D ratio, with no

clear evidence of structure aside from the prominent dust lane. At low surface brightness levels, the isophotes take on a pointy-box morphology typical of disk systems with boxy bulges.

NGC 5085.—SABbc: Small, bright bulge. Outer bulge isophotes are elliptical, but no other evidence of a bar. Grand-design two-armed spiral, with well defined, broad spiral arms. Arms can be traced nearly 360° before fading. Arm that emerges on the SW of the bulge bifurcates after winding almost 180°. Both arms have many star-forming knots, even quite far out in the disk.

NGC 5101.—(R)SB0/a: Bright nuclear point source embedded in a large, bright, circular bulge. At fainter isophotes the bulge becomes elliptical and is threaded by a thin, prominent bar. There are ansae at the ends of the bar that form the base of a ring/spiral arms. No evidence of star formation or structure in the disk.

NGC 5121.—S0: Bright nuclear point source. Inner bulge isophotes are circular but become elliptical at larger radii. No evidence for a bar. Very LSB disk with no evidence for internal structure.

NGC 5161.—SBab: Centrally condensed elliptical bulge embedded in a faint bar. Bright ansae are offset slightly downstream (assuming trailing arms) from the ends of the bar. Spiral pattern is two-armed, but the arms are patchy, diffuse, and fragmented. Arm features are clear for more than 180° of winding. The optical types for this galaxy are SA(s)c: (RC3), Sc(s)I (CAG), and Sc (OSU *B*). The substantially earlier type in the near-IR is due to the enhanced prominence of the bulge in the *H* band compared to the optical, and the low surface brightness of the outer, open arms in the near-IR.

NGC 5247.—Sc (type example—see Fig. 3*g*): Elliptical, centrally condensed bulge. No evidence of a bar. Inner HSB disk shows the origin of the two-armed grand-design spiral pattern. Spiral arms are very well defined, with numerous star-forming knots along their central ridge lines. Pattern is slightly asymmetric, with the north arm being more open and less extended than the south arm. Both arms bifurcate after wrapping for about 180°. The secondary arms are much fainter than the primary arms beyond the bifurcation.

NGC 5248.—Sb: Nuclear point source embedded in a short, wide nuclear bar. Nucleus/bar structure is further embedded in a luminous elliptical bulge with a P.A. skewed ~45° from that of the bar. Two well-defined, asymmetric spiral arms appear in the inner disk. The arms are rich in knots. The north arm turns through ~90° and then terminates abruptly. The surface brightness of the south arm drops after ~90° also, but the south arm can be traced beyond this point for another ~90° before fading from view. There are wispy, very LSB features in the outer disk, mainly on the west side.

ESO 383-G87.—dI (type example—see Fig. 3*k*): No bulge. No nucleus. No spiral structure. Diffuse LSB disk with an axial ratio of roughly 2 : 1. A large number of bright knots that could be star clusters or individual bright stars. The system appears to have an isophotal twist at large radii.

NGC 5334.—SBd: Small bulge embedded in a short, prominent bar. The bulge/bar system is surrounded by a wispy, irregular disk that has many spiral segments, but no coherent spiral arm pattern. The disk has a number of concentrations and knots in it.

NGC 5371.—SBbc: Nuclear point source embedded in an elliptical bulge. Bulge is threaded by a prominent bar with a P.A. skewed ~45° from that of the bulge. On the west side of the bar, a doubled arm emerges offset behind the end of the bar. The outer part of the doubled arm can be traced through ~400° before it fades into the sky. After ~270° it becomes smooth and LSB. On the east end of the bar a single arm emerges from the bar end, with no offset. The arm can be traced through ~90° before it merges with the inner part of the doubled west arm. The merged feature can be traced through another ~300° after this. For the last ~120°, it is smooth and LSB. The disk is full of knots, with the brightest knots in the arms. There are clear dust lanes especially on the southern side of the disk.

NGC 5427.—Sc: System is nearly face-on. Bright nucleus embedded in a small, slightly elliptical bulge. Some evidence for a weak oval distortion with a P.A. skewed by ~45 from that of the bulge. Grand-design two-armed spiral pattern emerges from the bulge. The arm that emerges from the west side of the bulge is HSB for ~250° and has many bright knots. It then fades, but it can be traced through a full 360° winding. The east arm has fewer knots and is HSB for only ~150°. It can also be traced at lower surface brightness levels through a full 360°. Both arms have spurs at ~180°. There is a LSB bridge to the interacting companion to the south.

NGC 5448.—SABa: System close to edge-on. Nuclear point source embedded in an elliptical bulge. Outer bulge isophotes are boxy, with a pronounced X-distortion at low levels. An LSB bar threads the bulge along its diagonal. Spiral arms begin at the ends of the bar. The bases of the arms are higher surface brightness than the ends of the bar and are also fairly broad. The broad, high-contrast portions of the arms are short. After only ~45°, the arms become narrow and much fainter. After ~90° the arms become fainter still and appear to bifurcate. The outer LSB arms are very diffuse. The inner arms appear to wrap around the disk, forming a nearly complete ring.

NGC 5483.—SBc: Small bulge embedded in a small lens/bar. Two smooth, well-defined spiral arms emerge from the ends of the bar. Arms emerge at right angles to the bar P.A. and can be traced for ~180° before fading. Inner arms have some evidence for knots, but outer arms are quite smooth. Arms become much wider and more diffuse at ~180°. P.A. of outer isophotes is ~90° offset from that of bar/lens component.

NGC 5530.—Not observed due to the presence of a very bright star superposed on the galaxy nucleus.

IC 4402.—Sc?: System close to edge-on. Small, bulge/nucleus, with no sign of a bar. There appear to be two main spiral arms, but they are quite asymmetric. The SE side of the galaxy is much brighter than the NW side. This may be due to the dust absorption features that are obvious even in the *H* band.

IC 4444.—(R)SB(r)cd: Star just north of nucleus. Small, faint bulge, threaded by well-defined bar. There appears to be a complete inner ring at the radius of the bar ends, but the star makes this difficult to determine. There are at least three spiral arms, all of which commence from the ends of the bar. The SE end of the bar has one arm emanating from it, winding to the west. This arm extends only 90° before it fades into the ambient disk. The NW end of the bar has two arms emanating from it. One is tightly wound, short, and full of bright star-forming knots. The other is quite loosely wound and wraps for ~180° before fading. This third arm

has a region of intense star formation roughly east of the bulge (winding angle of $\sim 120^\circ$).

NGC 5643.—SB(r)a: Bright nuclear point source, embedded in slightly elliptical bulge. Bulge is threaded by a narrow, prominent bar. Bar and bulge major axis are misaligned by $\sim 30^\circ$, but there is an isophotal twist in the bulge, such that the bar and bulge isophotes align at low intensity. Bright spiral arms begin at the ends of the bar. The spiral structure is flocculent and asymmetric, but features can be traced out for several windings. The arms are rich in star-forming knots, and filamentary structure.

NGC 5676.—SABbc: Small elliptical/boxy bulge threaded by a short, low-contrast bar. Two-armed spiral pattern emerges from the ends of the bar, at an angle of $\sim 150^\circ$ to the bar major axis. The arms are knotty and have a number of bends in them but are well defined, high-contrast features for almost a full 360°. Beyond this, the arm on the NE side of the galaxy stops abruptly. The arm on the SW side becomes broad and diffuse, fading into the outer disk. There are two short arm spurs on the SW side of the disk. These branch out from the arm that ends on the NE side of the galaxy.

NGC 5701.—(R)SB0: Bright centrally condensed nucleus embedded in a large, bright, slightly elliptical bulge. Bulge is threaded by a faint, diffuse bar, oriented parallel to the bulge major axis. Bulge/bar system is embedded in a faint disk. The disk is largely featureless, but there are a few objects that are either knots or companion galaxies. The disk may have a faint outer ring.

NGC 5713.—SBdm: System nearly face-on. Bright flattened nucleus, embedded in a short HSB bar. The bar has LSB extensions that are skewed from the main bar P.A. The disk is very asymmetric: There are three spiral arms, all of which emanate from the south side of the bar (bar is oriented close to E-W). The inner disk and inner arms are full of knots and HSB patches. These are much more prevalent on the south side of the bar. The arm structure can be traced through $\sim 270^\circ$ but becomes diffuse after the first $\sim 90^\circ$. The outer disk isophotes are not centered on the nucleus, but instead appear offset to the south.

NGC 5850.—SB(r)0/a (type example—see Fig. 3*b*): Elliptical nuclear source. The outer bulge isophotes are nearly circular. Bulge is threaded by a prominent and very long bar with a P.A. that is skewed by 60° with respect to that of the inner bulge. Bright ansae at the ends of the bar. Extensions from the ansae form a complete inner ring. After the ring is complete, these extensions continue, and become faint spiral features at larger radii. They appear to form an incomplete outer pseudoring as well.

NGC 5921.—SB(r)bc: Marginally resolved nucleus embedded in slightly elliptical bulge. Bulge is threaded by a prominent bar with a P.A. skewed by $\sim 30^\circ$ from the bulge major axis. A sharp inner ring encloses the bar. The ring is formed by two spiral arms that begin at the bar ends and nearly close together. Just before the ring would close, the arms become very open, broad, and diffuse. At the north end of the bar, the arm becomes brighter as it leaves the ring. The outer arms are asymmetric, with the west arm being shorter and more open.

NGC 5962.—SBab: Small, slightly elliptical bulge, threaded by a high-contrast bar. The bar P.A. is skewed $\sim 60^\circ$ from the bulge major axis. Spiral arms commence from the ends of the bar and form an almost complete inner pseudoring before opening. The arms are fairly low contrast and patchy. Past the ring, they can only be followed for $\sim 90^\circ$ before they fade into the outer disk. The outer disk has the same P.A. as the bulge.

NGC 6215.—SABbc: Small bulge is elliptical at high surface brightness, becoming circular at lower surface brightness levels. No other evidence of a bar. Diffuse two-armed spiral pattern emerges along the minor axis of the bulge. The arms are asymmetric, with the arm emerging on the south side of the bulge being the much higher surface brightness arm. There are some clear knots in the south arm. Both arms are doubled.

NGC 6221.—SBb: Nuclear point source embedded in slightly elliptical, moderately bright bulge. Bulge is threaded by a bar with an absorption band through it. The bar is aligned with the bulge minor axis. Two very open arms emerge from the ends of the bar. The arms have short HSB segments that are narrow and rich in knots. The north arm has a long, broad LSB continuation. The south arm seems to stop abruptly, but may continue at very LSB levels. The optical types for this galaxy are SB(s)c (RC3), Sbc(s)II–III (CAG), and SABcd (OSU *B*). The substantially earlier type in the near-IR is due to the heavy and irregular dust obscuration in the central part of the galaxy, which conceals much of the bulge visible in the *H* band.

ESO 138-G10.—S0: Heavy foreground contamination. Centrally condensed nucleus, surrounded by diffuse, featureless disk. There is one concentration of knots to the east, but this may be a dI companion. The optical types for this galaxy are SA(s)dm (RC3) and Sdm (OSU *B*). The radically earlier type in the near-IR is due to the smooth, featureless appearance of the disk in the *H* band.

NGC 6300.—SB(r)a: Slightly elliptical nucleus, and bulge. Strong bar is skewed to bulge major axis by $\sim 45^\circ$. Bar intersects a ring/tight arms. Bright ansae at the intersections. Ring/arms are patchy but fairly well defined. Ring/arms clearly have many knots, despite obvious contamination by foreground stars. The optical types for this galaxy are SB(rs)b (RC3), SBb(s)II pec (CAG), and SAB(r)bc (OSU *B*). The substantially earlier type in the near-IR is due to the enhanced prominence of the bulge in the *H* band compared to the optical.

NGC 6384.—SBbc: Very elliptical bulge threaded by a short, prominent bar. The bulge isophotes show a clear (if small) isophotal twist such that the outer bulge isophotes are aligned with the bar major axis. The bulge/bar system is embedded in a lens, with a flocculent spiral pattern emerging from the lens. A large number of armlets are visible. The armlets are typically smooth, with no strong evidence of knots or dust lanes.

NGC 6753.—Sa: Bright nuclear point source, embedded in slightly elliptical bulge. No sign of a bar. Bulge is embedded in a lens. Beyond the lens, there are a number of faint, tightly wrapped spiral arms embedded in a LSB disk. Very few star-forming knots visible.

NGC 6782.—(R)SB0/a: Bright, centrally condensed bulge. Nuclear region of bulge is elliptical (major axis oriented NE-SW) but embedded in a circular bulge. Prominent bar oriented nearly N-S. Weak ansae at the ends of the bar signal a faint inner disk. Inner disk is quite elliptical, with the same major axis P.A. as the bar. Evidence for a much fainter outer disk that is nearly circular. Arclike features to the south appear to be due to scattered light from a bright star.

ESO 142-G19.—Sa?: Nearly edge-on. Bright nuclear point source embedded in a large, luminous bulge. Bulge is cut on the west side by a prominent absorption lane. A thin, well-defined disk extends from the bulge major axis. The absorption band can be traced out into this disk. There appear to be a few knots of star formation in the inner disk.

NGC 6902.—SB(r)a: Bright, circular, centrally condensed bulge. Bright bar oriented NW-SE. Two-armed spiral pattern, with arms emerging from ends of the bar and wrapping tightly counterclockwise. Arms fade drastically after 180° but continue for more than a full turn at low surface brightness. Inner arms appear to form an inner pseudoring.

NGC 6907.—SBbc: Two-armed, grand-design spiral. May be influenced by companion that is superposed on NE arm. Bulge is elliptical, and skewed with respect to the arms (inner "arms" may be a bar): The bulge major axis is offset nearly 45° from the base of the arms. Inner arms are well defined and have a number of bright knots in them. Knots apparent to much larger distances along NE arm, possibly due to interaction with the projected companion. At low light levels, the arms wrap entirely around the galaxy to form an outer pseudoring.

IC 5052.—Sd: System edge-on. No evidence of a bulge, or of spiral structure. Despite the edge-on orientation, there is no sign of any prominent dust lane. The system is oriented NW-SE; the NW side has a much higher surface brightness than the SE side. There are obvious knots throughout the disk. Again, these are more prevalent on the NW side.

NGC 7083.—Sb: Bright, centrally condensed bulge. Inner bulge is circular but becomes quite elliptical at larger radii. Two-armed grand-design spiral pattern with the arms beginning at the bulge minor axis. The arms each have a single dominant ridge line and many fainter ones. The arms both bifurcates immediately, with the brighter parts wrapping more tightly. These HSB portions wrap for ~120°. The outer, LSB arms can be followed for at least 270°. They are patchy and have multiple armlets and filaments. There is obvious star formation very far out.

NGC 7184.—SB(r)a: Bright pointlike nucleus. Elliptical bulge, with major axis aligned with the disk major axis. A bar appears oriented perpendicular to the bulge, although the high inclination makes this uncertain. As the bulge isophotes become more circular, they connect with a bright ring, formed from tightly wrapped spiral arms. Arms are fairly smooth. Isophotes indicate that the arms begin on the SE and NW sides of the bulge, and sweep around to the NE and SW, respectively. More arm features, at lower surface brightness, continue beyond the ring.

NGC 7205.—SABb (type example—see Fig. 3*e*): Evidence for weak a bar. Grand-design spiral pattern that makes at least a full winding. Arm that originates from the SW side of the bulge is more clearly defined. Both arms show evidence of bifurcation/rattiness after about 180°.

NGC 7213.—S0 (type example—see Fig. 3*a*): Very bright nuclear point source embedded in a circular bulge. Disk fills the frame but is very faint and featureless.

NGC 7217.—S0/a (type example—see Fig. 3*b*; see Fig. 4*b*): Bright nucleus embedded in very prominent, slightly elliptical bulge. No evidence of a bar. Faint disk extends beyond bulge, with just a hint of wispy spiral structure in the disk. Note in Figure 4*b* that there is clear outer arm structure visible in the *B* band. This indicates the arms are regions of active star formation, rather than being dust arms.

NGC 7314.—No *JHK* data.

NGC 7410.—No *JHK* data.

NGC 7412.—SABc (type example—see Fig. 3*g*): Small, centrally condensed, slightly elliptical bulge. Bulge is embedded in a smooth inner disk. A grand-design two-armed spiral pattern emerges from the inner disk, with the arm origins aligned with the bulge major axis. Both arms bifurcate. The north arm has a great deal of structure in its inner part. There is a faint galaxy that may be a companion superposed on the very inner part of the north arm. The arm bifurcates after ~60°, with the higher surface brightness part wrapping tightly. The HSB part can be traced for another 90°. The LSB part is very loosely wrapped but can still be traced for another 90°. The south arm has much less inner structure. It also bifurcates, but after only ~30°. The inner part is also the HSB part, but here the HSB part can be traced for ~150° before fading. The LSB part fades after only ~60°. The LSB south arm shows clear evidence for current star formation.

NGC 7418.—SBbc (see Fig. 4*f*): Bright point source nucleus embedded in a strong bar. Complex, multiarm spiral with arms beginning around bar ends. At least four arms are well enough defined to call such. Inner parts of arms have many bright knots. Outer arms are fairly smooth. Note in Figure 4*f* that the spiral arms are very blue, but the bar is a mix of green (*R* band) and red (*H* band). Optical classifications of this galaxy are unbarred or weakly barred, while it is strongly barred at *H*.

IC 5267.—No *JHK* data.

IC 5271.—No data.

IC 5273.—No data.

NGC 7479.—(R)SBbc: Strong, thin bar, at a P.A. slightly skewed from the bulge major axis P.A. Bar is close to N–S. Bulge is elliptical. Arms come from ends of the bar but are not perpendicular to the bar. South arm commences with a sharp west kink at the end of the bar. Second kink to the north, and then a smooth curve until the arm fades after roughly 180°. North arm emerges smoothly from bar and curves smoothly back to the south. Also fades after ~180°. Arms appear to form an off-center pseudoring. South arm is more open than the north arm (thus, the bulge is to the east of the center of the pseudoring).

NGC 7496.—No data.

NGC 7513.—No data.

NGC 7552.—(R)SBa: Irregular nuclear region. At lower intensity, bulge becomes regular and elliptical. Prominent, long bar aligned with bulge major axis. Bar surface brightness is irregular, with several knots/lumps of enhanced brightness. Bar appears to end in points, with faint, very open spiral arms emerging from the bar ends. The arms are quite smooth, with few knots or irregularities. At low surface brightness levels, the winding of the arms tightens, and they wrap at least 180° around the galaxy.

NGC 7582.—(R)SBb?: Bright nuclear point source embedded in large bulge. System is nearly edge-on. The inner bulge isophotes are elliptical. At lower intensity, the bulge has a strong "X" feature. The high inclination makes any spiral pattern impossible to detect. However, there is obvious structure in the disk, with clumps of star formation, and dust obscuration visible. No coherent dust lanes are apparent. At low surface brightness levels, the X structure resembles a peanut bulge, and the disk shows a pronounced integral-sign warp. There are very LSB spiral features extending from the disk and wrapping nearly entirely

around the galaxy. These features are broad and smooth, with no sign of internal structure.

NGC 7606.—Sab (type example—see Fig. 3*d*): No sign of a bar. Bright nuclear point source extends into prominent elliptical bulge (ellipticity appears due to inclination). Generally two-armed pattern, but with several arm fragments. Arms are fairly smooth, with only a few bright knots. Possible to trace arms nearly a full 360°.

IC 5325.—SABbc (type example—see Fig. 3*f*): Nearly face-on. Bulge is circular at high light levels but shows signs of an oval distortion at lower light levels. Flocculent spiral pattern, with four significant arms. Two most prominent arms originate at the major-axis ends of the oval distortion. West arm is higher surface brightness than the others.

NGC 7713.—Sdm (type example—see Fig. 3*j*): No true bulge. Nuclear point source embedded in very elliptical disk. Disk ellipticity appears due to inclination, rather than a bar. The HSB part of disk is not centered on the nucleus (the nucleus is north of the center of the inner disk). No clear spiral pattern in the disk, although there are many star-forming knots. The LSB part of the disk is not centered on the HSB disk but is more extended to the north (in the opposite sense of the offset between the nucleus and the HSB disk). The LSB disk is irregular in shape and has a number of filamentary structures in it.

NGC 7723.—SB(r)ab: Bright, symmetric nucleus, embedded in a boxy bulge, and threaded by a thin HSB bar. Bar emerges from opposite corners of the boxy bulge. Bar terminates abruptly, and arms emerge to form an inner pseudoring. Arm structure is very complex. One arm emerges from the SW end of the bar, with an opening angle of ~45°, and winds to the NE. It is well defined for ~90° and then becomes fat and diffuse. The pitch angle increases at this point. This arm fades into the general disk after winding for ~180°. The arm associated with the NE end of the bar does not begin at the bar. Instead, it begins as a diffuse feature ~60° NW of the bar end and brightens until it reaches the bar end. It then bifurcates. The inner (generally higher surface brightness) portion forms the SW part of the pseudoring. This inner portion bifurcates again after winding ~120° from the bar end. Once again, the inner portion forms the pseudoring. And after this second bifurcation the inner arm brightens, before fading and diffusing into the general disk. After both bifurcations, the outer arms are very diffuse, LSB features that wind for ~90° before fading. There are no obvious star-forming knots.

NGC 7727.—S pec (early): Elliptical nuclear source embedded in a boxy (rhomboid) bulge. Bulge is very large. Four faint, broad, irregular arms emerge from the bulge. These arms have differing pitch angles and extents. Some can be followed through more than 90° of winding. Some stop very quickly. Several large-scale LSB features are visible. Merger remnant?

NGC 7741.—SBcd: No true bulge. Inner bar resolved into two sources at high surface brightness levels. There are many star-forming knots, mainly in the spiral arm features. The arms are patchy and diffuse. The inner arms form an inner pseudoring. Outside of this ring, the arms are even more diffuse and have spokelike filamentary structure.

NGC 7814.—S0/a: Edge-on system. Bright nuclear point source embedded in a large, luminous, flattened bulge, cut by an obvious dust lane along the major axis. The disk is very thin and imposed on the much brighter bulge. There is no evidence for spiral structure, due to the inclination of the disk. There is no evidence for star formation. Only the presence of the dust lane prevents a classification of S0.

5. SUMMARY AND DISCUSSION

We have presented optical (*B* band) and near-IR (*H* band) morphological classifications for a statistically complete sample of ≈200 bright spiral galaxies. Our optical classifications agree well with those of the standard catalogs (see Figs. 2*a*–2*c* and Tables 2A–2C). The mean absolute difference between our optical classifications and those from both the RC3 and the CAG is about half a T type, with no evidence for any systematic differences beyond those already known to exist in the two standard optical catalogs. Our *H*-band classifications average about 1 T type earlier than our optical classifications and the optical classifications from both the RC3 and the CAG (see Figs. 2*d*–2*f* and Tables 2D–2F). There is thus a clear tendency for spiral galaxies to appear somewhat earlier-type in the near-IR than in the optical, but with large scatter. Our results thus do not support the assertion of Block & Puerari (1999) that the optical and near-IR morphologies of spiral galaxies are "decoupled." On average, there is quite a good correlation between the optical and near-IR morphology of spirals, although there are cases that show dramatic differences.

We have given short descriptions of the *H*-band morphology of our sample. We have also presented *B*- and *H*-band images of a set of galaxies, selected as examples of their *H*-band morphological type. In addition, we have presented false-color (*BRH*) images of six galaxies ranging from early- to late-type spirals, three of which look essentially the same in the optical and the near-IR, and three of which look substantially different.

The OSU Survey is an important tool for studies of the properties of spiral galaxies in the nearby universe. The broad wavelength coverage and the large, well-defined, and statistically complete sample invites a wide range of studies on the morphology, dynamics, ISM, and stellar populations of spiral galaxies. The sample also provides a template to compare with samples of galaxies at high redshift. Data from the OSU Survey have already contributed to a number of results in studies of galaxy morphology (Terndrup et al. 1994; Quillen et al. 1997; Eskridge et al. 2000; Elmegreen et al. 2002; Whyte et al. 2002), galaxy dynamics (Quillen, Frogel, & Gonzalez 1994; Quillen et al. 1995; Patsis, Athanassoula, & Quillen 1997; Quillen & Frogel 1997; Puerari et al. 2000), galaxy evolution (van den Bergh et al. 2002), and dust and extinction (Kuchinski & Terndrup 1996; Berlind et al. 1997; Kuchinski et al. 1998).

We are engaged in a number of collaborative projects using the OSU Survey data. It is particularly important to extend the qualitative study we have done in this paper to more quantitative studies of galaxy morphology. This work will place our understanding of the properties of current spiral galaxies on a firmer physical footing and allow for a realistic comparison between the galaxy populations of the low- and high-redshift universe. We are engaged in a collaboration to apply the "Hubble-space" analysis of Abraham & Merrifield (2000) to the OSU sample (van den Bergh et al. 2002; Whyte et al. 2002). As the OSU sample is complete and well defined, it provides for a much better assessment of local galaxy properties than does the sample used by Abraham & Merrifield (2000). The application of the "Hubble-space" analysis to our sample allows a better

analysis of the claim (Abraham et al. 1999b) that the bar fraction of disk galaxies is a strong function of redshift (van den Bergh et al. 2002). A related project that we are pursuing is a comparative study of a number of the various quantitative measures of "bar strength" that exist in the literature (e.g., Elmegreen & Elmegreen 1985; Abraham et al. 1999; Buta & Block 2001; Odewahn et al. 2002).

The pixel-mapping technique of Abraham et al. (1999a) is a powerful tool for studying the star formation history of nearby galaxies. Application of this technique to a large sample of the OSU survey will result in a more detailed understanding of the relationship between the morphology and star formation histories of galaxies along the Hubble sequence. Galaxy asymmetry studies are also proving to be important means of probing the connection between star formation history and dynamical evolution in disk galaxies (Conselice, Bershady, & Jangren 2000). The OSU survey provides an excellent zero-redshift benchmark for such studies.

It would be especially interesting to apply the methodology of the "dust-penetrated" classification scheme of Block & Puerari (1999) to *both* our optical and near-IR data. We could then carry out a quantitative assessment of the qualitative results of the current study (that spiral galaxies are, on average, slightly earlier type in the near-IR that in the optical). Another related program we are engaged in is a comparison of the optical and IR properties of anemic and normal spirals (Elmegreen & Elmegreen 1987; Elmegreen et al. 2002).

Galaxy evolution has become a practical observational study in the last decade. But the sort of detailed morphological work that is possible for samples of hundreds of galaxies, each hundreds of resolution elements across is simply impossible for samples of tens of thousands of galaxies, each tens of resolution elements across. The OSU sample provides a zero-redshift benchmark for comparison with high-redshift galaxy samples. We are involved in collaborations to apply both the "Hubble-space" and pixel-mapping techniques of Abraham and collaborators (Abraham et al. 1999a; Abraham & Merrifield 2000), and the neural-net techniques of Odewahn and collaborators (Odewahn et al. 1996, 2002) to the OSU Sample. It is an irony of modern studies of galaxy evolution that high-redshift galaxy samples are better defined and better observed than zero-redshift samples. The availability of the OSU Sample helps to rectify this paradoxical situation.

The broad wavelength coverage of the OSU Survey invites extensions to other wavelength regimes. A number of the galaxies in our sample are part of the BIMA/SONG sample (Regan et al. 2001). It is a natural question to ask how the distribution of molecular gas in these galaxies correlates with the distribution of both the young stellar populations (as traced by the *B* band) and the old stellar populations (as traced by the *HK* bands). Extension of the Survey observations into the vacuum ultraviolet both allows the study of the youngest stellar populations and provides a firmer footing for comparisons with the rest-frame UV observations of distant galaxies from the *Hubble Space Telescope* (*HST*). We have begun such a program for a few of the galaxies in the OSU Survey (Eskridge et al. 2001), however, the small field of the of the WFPC2 on *HST* has restricted this work to the smallest systems in the survey. The coming availability of the wider-field Advanced Camera for Surveys will allow us to extend the observations to a much larger fraction of the Survey galaxies.

The approaching launch of SIRTF will provide an opportunity to extend the wavelength baseline for the OSU survey through the infrared. It will be possible to obtain well-resolved images for the OSU sample with IRAC in the range of 3–8 μm, and marginally resolved images, and total fluxes for the longer wavelengths with MIPS. This will allow for a much better understanding of the detailed physical processes relating the stellar populations and the ISM in spirals.

The study of galaxy morphology has been a crucial tool for our understanding of the universe for the last 80 years We are now entering an era when the early qualitative, single waveband approach to morphology is maturing into a quantitative, multiwavelength discipline. Our understanding of the structure, evolution, and underlying physics of galaxies will advance with our ability to study their properties across the electromagnetic spectrum and along the evolutionary axis of redshift. We believe the OSU Survey will play an important role in this advance.

We thank the many OSU graduate students who collected data for this project, and we wish to especially note the many nights of work that Ray Bertram and Mark Wagner have devoted to the OSU Survey. We are grateful to Roberto Aviles for obtaining many of the optical images of southern galaxies for us with the 0.9 m telescope at CTIO. We thank Bob Williams and Malcolm Smith, past and present directors of CTIO, for the generous allotment of telescope time needed to observe most of our southern sample. We happily acknowledge the work of the builders of OSIRIS and the IFPS, especially Bruce Atwood, Tom O'Brien, and Paul Byard of the OSU Imaging Sciences Laboratory. J. A. F. thanks Leonard Searle for the observing opportunities provided by a Visiting Research Associateship at Las Campanas Observatory, where some of these data were obtained. We are pleased to thank Ron Buta and Allan Sandage for several very useful discussions on galaxy morphology. Our referee did an outstanding job of catching many of the errors and weaknesses in the original manuscript. J. A. F. acknowledges support from a PPARC Senior Visiting Research Fellowship (grant GR/L00896) held in 1996 at the University of Durham Physics Department. The construction of the IFPS was supported by grants AST-8822009 and AST-9112879 from the National Science Foundation. The construction of OSIRIS was supported by grant AST-9016112 from the National Science Foundation. This work was supported by grants AST-9217716 and AST-9617006 from the National Science Foundation.

REFERENCES

Abraham, R. G., Ellis, R. S., Fabian, A. C., Tanvir, N. R., & Glazebrook, K. 1999a, MNRAS, 303, 641
Abraham, R. G., & Merrifield, M. R. 2000, AJ, 120, 2835
Abraham, R. G., Merrifield, M. R., Ellis, R. S., Tanvir, N. R., & Brinchmann, J. 1999b, MNRAS, 308, 569
Abraham, R. G., Valdes, F., Yee, H. K. C., & van den Bergh, S. 1994, ApJ, 432, 75
Berlind, A. A., Quillen, A. C., Pogge, R. W., & Sellgren, K. 1997, AJ, 114, 107
Block, D. L., Bertin, G., Stockton, A., Grosbøl, P., Moorwood, A. F. M., & Peletier, R. F. 1994, A&A, 288, 365
Block, D. L., & Puerari, I. 1999, A&A, 342, 627
Block, D. L., & Wainscoat, R. J. 1991, Nature, 353, 48
Buta, R. 1986, ApJS, 61, 609

Buta, R. 1995, ApJS, 96, 39
Buta, R., & Block, D. L. 2001, ApJ, 550, 243
Conselice, C. J., Bershady, M. A., & Jangren, A. 2000, ApJ, 529, 886
DePoy, D. L., Atwood, B., Byard, P. L., Frogel, J., & O'Brien, T. P. 1993, Proc. SPIE, 1946, 667
de Vaucouleurs, G. 1959, Handb. Phys., 53, 275
de Vaucouleurs, G., de Vaucouleurs A., & Corwin, H. G., Jr. 1976, Second Reference Catalogue of Bright Galaxies (Austin: Univ. Texas Press)
de Vaucouleurs, G., de Vaucouleurs A., Corwin, H. G., Jr., Buta, R. J., Paturel, G., & Fouqué, P. 1991, Third Reference Catalogue of Bright Galaxies (Springer: New York) (RC3)
Elmegreen, B. G., & Elmegreen, D. M. 1985, ApJ, 288, 438
Elmegreen, D. M., & Elmegreen, B. G. 1982, MNRAS, 201, 1021
———. 1987, ApJ, 314, 3
Elmegreen, D. M., Elmegreen, B. G., Frogel, J. A., Eskridge, P. B., Pogge, R. W., Gallagher, A., & Iams, J. 2002, AJ, 124, 777
Eskridge, P. B., et al. 2000, AJ, 119, 536
———. 2001, BAAS, 33, 1379
Frei, Z., Guhathakurta, P., Gunn, J. E., & Tyson, J. A. 1996, AJ, 111,174
Hackwell, J. A., & Schweizer, F. 1983, ApJ, 265, 643
Hubble, E. P. 1936, The Realm of the Nebulae (New Haven: Yale Univ. Press)
Kuchinski, L. E., & Terndrup, D. M. 1996, AJ, 111, 1073
Kuchinski, L. E., Terndrup, D. M., Gordon, K. D., & Witt, A. N. 1998, AJ, 115, 1438
Mayr, E. 1942, Systematics and the Origin of Species (New York: Columbia Univ. Press)
Morgan, W. W. 1958, PASP, 70, 364
Morgan, W. W., Kayser, S., & White, R. A. 1975, ApJ, 199, 545
Naim, A., Ratnatunga, K. U., & Griffiths, R. E. 1997, ApJS, 111, 357
Naim, A., et al. 1995, MNRAS, 274, 1107
Odewahn, S. C., Cohen, S. H., Windhorst, R. A., & Philip, N. S. 2002, ApJ, 568, 539
Odewahn, S. C., Windhorst, R. A., Driver, S. P., & Keel, W. C. 1996, ApJ, 472, L13
Parsons, W. 1850, MNRAS, 10, 21
Patsis, P. A., Athanassoula, E., & Quillen, A. C. 1997, ApJ, 483, 731
Pogge, R. W., et al. 1998, Proc. SPIE, 3354, 414
Puerari, I., Block, D. L., Elmegreen, B., Frogel, J. A., & Eskridge, P. B. 2000, A&A, 359, 932
Quillen, A. C., & Frogel, J. A. 1997, ApJ, 487, 603
Quillen, A. C., Frogel, J. A., & Gonzalez, R. A. 1994, ApJ, 437, 162
Quillen, A. C., Frogel, J. A., Kenney, J. D. P., Pogge, R. W., & DePoy, D. L. 1995, ApJ, 441, 549
Quillen, A. C., Kuchinski, L. E., Frogel, J. A., & DePoy, D. L. 1997, ApJ, 481, 179
Regan, M. W., Thornley, M. D., Helfer, T. T., Sheth, K., Wong, T., Vogel, S. N., Blitz, L., & Bock, D. C.-J. 2001, ApJ, 561, 218
Rhoads, J. E. 1998, AJ, 115, 472
Sandage, A. 1961, The Hubble Atlas of Galaxies (Washington: Carnegie Inst. Washington)
Sandage, A., & Bedke, J. 1994, The Carnegie Atlas of Galaxies (Washington: Carnegie Inst. Washington) (CAG)
Schweizer, F. 1976, ApJS, 31, 313
Terndrup, D. M., Davies, R. L., Frogel, J. A., DePoy, D. L., & Wells, L. A. 1994, ApJ, 432, 518
Thronson, H. A., Jr., et al. 1989, ApJ, 343, 158
van den Bergh, S. 1976, ApJ, 206, 883
van den Bergh, S., Abraham, R. G., Whyte, L. C., Merrifield, M. R., Eskridge, P. B., Frogel, J. A., & Pogge, R. W. 2002, AJ, 123, 2913
Whitmore, B. C., & Bell, M. 1988, ApJ, 324, 741
Whyte, L. F., Abraham, R. G., Merrifield, M. R., Eskridge, P. B., Frogel, J. A., & Pogge, R. W. 2002, MNRAS, in press (astro-ph/0207461)
Zwicky, F. 1955, PASP, 67, 232